Science of the Total Environment 768 (2021) 144278

Contents lists available at ScienceDirect

Science of the Total Environment

journal homepage: www.elsevier.com/locate/scitotenv

Modelling the interplay of future changes and wastewater management measures on the microbiological river water quality considering safe drinking water production

Katalin Demeter [a,b,1,2], Julia Derx [c,1,2], Jürgen Komma [c], Juraj Parajka [c], Jack Schijven [d,e], Regina Sommer [f,1], Silvia Cervero-Aragó [f,1], Gerhard Lindner [f,1], Christa M. Zoufal-Hruza [g], Rita Linke [a,1], Domenico Savio [h,1], Simone K. Ixenmaier [a,1], Alexander K.T. Kirschner [f,1], Harald Kromp [i], Alfred P. Blaschke [c,1], Andreas H. Farnleitner [a,h,*,1]

[a] Institute of Chemical, Environmental and Bioscience Engineering E166/5/3, TU Wien, Gumpendorferstraße 1a, A-1060 Vienna, Austria
[b] Center for Water Resource Systems E222, TU Wien, Karlsplatz 13, A-1040 Vienna, Austria
[c] Institute of Hydraulic Engineering and Water Resources Management E222/2, TU Wien, Karlsplatz 13, A-1040 Vienna, Austria
[d] Department of Statistics, Informatics and Modelling, National Institute for Public Health and the Environment (RIVM), PO Box 1, 3720 BA Bilthoven, the Netherlands
[e] Faculty of Geosciences, Department of Earth Sciences, Utrecht University, the Netherlands
[f] Institute for Hygiene and Applied Immunology, Medical University of Vienna, Kinderspitalgasse 15, A-1090 Vienna, Austria
[g] Division of Hygiene, Municipal Department 39, City Administration Vienna, Rinnböckstraße 15/2, A-1110 Vienna, Austria
[h] Division Water Quality and Health, Department of Pharmacology, Physiology, and Microbiology, Karl Landsteiner University of Health Sciences, Dr.-Karl-Dorrek-Straße 30, A-3500 Krems an der Donau, Austria
[i] Vienna Water, City Administration Vienna, Grabnergasse 4-6, A-1060 Vienna, Austria

HIGHLIGHTS

- Coupling of hydrologic & QMRA modelling to inform drinking water safety management
- Extended, open-source fate and transport model QMRAcatch calibrated on MST marker
- Dual approach (source apportionment and risk assessment) proved important
- Strong climate change effect if CSOs are major pollutants (enhanced WWTP treatment)
- Effects of future change and pollution control are site-and scenario-specific.

GRAPHICAL ABSTRACT

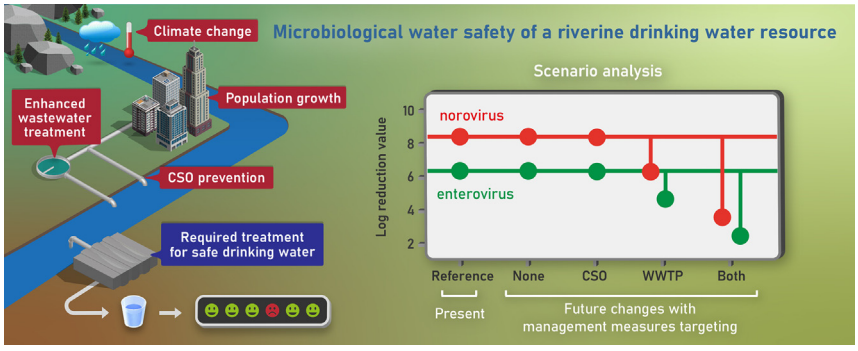

ARTICLE INFO

Article history:
Received 18 September 2020
Received in revised form 26 November 2020
Accepted 27 November 2020
Available online 24 December 2020

Editor: Damia Barcelo

ABSTRACT

Rivers are important for drinking water supply worldwide. However, they are often impacted by pathogen discharges via wastewater treatment plants (WWTP) and combined sewer overflows (CSO). To date, accurate predictions of the effects of future changes and pollution control measures on the microbiological water quality of rivers considering safe drinking water production are hindered due to the uncertainty of the pathogen source and transport variables. The aim of this study was to test an integrative approach for an improved understanding of these effects, i.e. climate change and population growth as well as enhanced treatment at WWTPs and/or prevention of CSOs. We applied a significantly extended version of QMRAcatch (v1.0 Python), a probabilistic-

* Corresponding author at: Division Water Quality and Health, Department of Pharmacology, Physiology, and Microbiology, Karl Landsteiner University of Health Sciences, Dr.-Karl-Dorrek-Straße 30, A-3500 Krems an der Donau, Austria.
E-mail address: andreas.farnleitner@kl.ac.at (A.H. Farnleitner).
[1] Interuniversity Cooperation Centre Water & Health (www.waterandhealth.at).
[2] These authors contributed equally.

https://doi.org/10.1016/j.scitotenv.2020.144278
0048-9697/© 2020 The Authors. Published by Elsevier B.V. This is an open access article under the CC BY-NC-ND license (http://creativecommons.org/licenses/by-nc-nd/4.0/).

Keywords:
Human-associated MST
Reference pathogens
Fate and transport model
Climate change
Quantitative microbial risk assessment

deterministic model that combines fate and transport modelling with quantitative microbial infection risk assessment. The impact of climatic changes until the period 2035–2049 was investigated by a conceptual semi-distributed hydrological model, based on regional climate model outputs. QMRAcatch was calibrated and validated using site- and source-specific data (human-associated genetic microbial source tracking marker and enterovirus). The study showed that the degree to which future changes affect drinking water safety strongly depends on the type and magnitude of faecal pollution sources and are thus highly site- and scenario-specific. For example, if the load of pathogens from WWTPs is reduced through enhanced treatment, climate-change driven increases in CSOs had a considerable impact. Preventing CSOs and installing enhanced treatment at the WWTPs together had the most significant positive effect. The simultaneous consideration of source apportionment and concentrations of reference pathogens, focusing on human-specific viruses (enterovirus, norovirus) and cross-comparison with bacterial and protozoan pathogens (*Campylobacter*, *Cryptosporidium*), was found crucial to quantify these effects. While demonstrated here for a large, wastewater-impacted river, the approach is applicable at other catchments and pollution sources. It allows assessing future changes and selecting suitable pollution control measures for long-term water safety planning.
© 2020 The Authors. Published by Elsevier B.V. This is an open access article under the CC BY-NC-ND license (http://creativecommons.org/licenses/by-nc-nd/4.0/).

1. Introduction

Rivers are important for drinking water supply worldwide, yet, they are often under pressure from multiple pollution sources. The most widespread health risk associated with drinking water is contamination with pathogens that originate from faecal matter (WHO, 2017b). In densely populated large river catchments, discharges of municipal wastewater treatment plants (WWTP) and combined sewer overflows (CSO) are major contributors to the faecal pollution load (Rickert et al., 2016; WHO, 2017b). Additional faecal pollution sources include wildlife and domestic animal waste. Understanding this plethora of pressures and their future changes, along with their impact on the drinking water source, poses a great challenge for water safety planning (Rickert et al., 2016).

The future climatic and population changes may affect faecal pollution sources, the microbiological quality of surface water, and ultimately drinking water safety. Population growth and the associated increase in (treated) wastewater discharges may result in the deterioration of river water quality, and the concerns may be further aggravated by climatic changes (WHO, 2017a). According to climate projections, the frequency and intensity of extreme rainfall events will increase in many areas (Myhre et al., 2019). This will result in runoff flushes and, in places with a combined sewer system, more frequent and intense CSO events (Bi et al., 2015; Nie et al., 2009; Willems et al., 2012). In addition, the hydrological regimes and temperatures of rivers are likely to change (e.g., Blöschl et al., 2019), affecting their buffering capacities in terms of dilution and inactivation of pathogens. Droughts and the resulting low river discharges would concentrate contaminants in river and groundwater resources (WHO, 2017a), while floods are often accompanied by short-term deteriorations of water quality due to agricultural runoff and CSOs (e.g., Derx et al., 2013). In contrast, higher water temperatures expected due to climate change may facilitate the inactivation of enteric pathogens (Boehm et al., 2019). If the pollution sources are mainly urban wastewater discharges, possible strategies to reduce faecal contamination include enhanced wastewater treatment and CSO prevention. As a final step in wastewater treatment, ozonation and advanced oxidation processes as well as UV-treatment and chlorination allow a considerably reduced pathogen load in the final effluent. Measures to prevent CSOs include reservoirs or any form of green infrastructure affecting runoff water quantity and quality at different spatial scales (Golden and Hoghooghi, 2018).

The sum of climatic and demographic changes were previously found to deteriorate microbiological water quality to a limited degree, with less than 0.5 $\log_{10}$ increase in the mean concentration of faecal indicator bacteria or index pathogens until 2040–2070, as shown for large rivers in Canada (Jalliffier-Verne et al., 2017; Jalliffier-Verne et al., 2015), Bangladesh (Islam et al., 2018a), Pakistan (Iqbal et al., 2019), and a fictive river in the Netherlands (Sterk et al., 2016). The impact of CSOs and WWTPs on the microbiological water quality of rivers has been analysed from various perspectives. Upstream short-term pollution events, such as via CSO discharges (Taghipour et al., 2019) or WWTP bypass and pumping station overflow events (Sokolova et al., 2015) were shown to be less important for drinking water safety if relying on surface water than the optimal treatment performance of the drinking water treatment plant itself. The simultaneous reduction of multiple faecal inputs in two catchments with high human population and livestock numbers was found beneficial under a sustainable future scenario, in comparison with the uncontrolled future scenario (Iqbal et al., 2019; Islam et al., 2018a). Medema and Schijven (2001) calculated that the majority of *Cryptosporidium* oocysts in Dutch rivers originates from treated sewage, while *Giardia* was rather linked to untreated discharges, pointing at the different strategies needed to reduce their concentrations in river water. Sterk et al. (2016) found an elevated infection risk through bathing downstream of the discharge point of a WWTP all-year round, while even higher risks, although intermittent, downstream of a CSO. The various measures that can be taken to reduce the input of pathogens into the river have not yet been analysed systematically. Questions also remain as to how climate and demographic changes would alter the effect of these measures.

Assessing faecal pollution dynamics and their possible future developments at the catchment scale is a complex problem as it involves large uncertainties of the source and transport variables (Cho et al., 2016). Most of these microbial fate and transport models focus on faecal indicator organisms (Islam et al., 2018b; Kim et al., 2017), while some also include microbial source tracking markers (MST) enabling source-specific model calibration (Sokolova et al., 2012) or pathogens allowing the assessment of health risks directly (Dorner et al., 2006; Fauvel et al., 2017). Depending on the purpose, the developments range from physically based models that simulate water currents requiring much computational effort, to process based pathogen fate and transport models requiring a high number of input parameters (e.g., SWAT, Kim et al., 2017). Recently, studies have combined fate and transport models with quantitative microbial risk assessment (QMRA) to estimate the health risk associated with drinking (Sokolova et al., 2015) or bathing (Eregno et al., 2016; Sterk et al., 2016). QMRAcatch was one of the first models of this kind. Its microbial fate and transport module follows a mass balance approach to simulate microbial concentrations in river water and accounts for the uncertainty of model input variables (e.g., concentration of microorganism in raw wastewater) by using a probabilistic approach. The QMRA module of QMRAcatch simulates the infection risks associated with the ingestion of pathogens contained in drinking water as well as the required treatment to produce safe drinking water (Derx et al., 2016; Schijven et al., 2015).

This study aimed to test a new integrative approach for deciphering the interplay between the effects of climate and demographic changes

and wastewater management measures on the microbiological river water quality with regards to the required treatment to produce safe drinking water. We investigated the effects of future climatic and demographic changes up to 2050, as 'no management changes' scenario, as well as these effects combined with measures that aim to reduce the pollution from upstream WWTPs, CSOs, or both. Additionally, we investigated the effects of increased CSOs in a systematic sensitivity analysis. The approach was tested at a Danube River study site in Vienna, representative of large rivers where the dominant source of faecal pollution is human wastewater from upstream point sources. The scenarios were analysed for two viral reference pathogens: enterovirus and norovirus, which are mainly associated with human wastewater and are often used as references for infection risk assessment from water resources (WHO, 2017b). Additionally, the scenarios were extended for *Campylobacter* and *Cryptosporidium* for a cross-comparison between human viral pathogens and bacterial and protozoan reference pathogens. To meet our aim, we significantly extended QMRAcatch (Schijven et al., 2015) (v1.0 Python) now available as open source, which we calibrated and validated based on concentrations of a human-associated genetic MST marker and infectious enteric viruses, measured at the study site monthly over a period of four years. In the scenario analysis, river discharges were simulated using a conceptual semi-distributed hydrological model and four regional climate model projections covering the range of expected climate change pathways.

2. Materials and methods

2.1. Study area

The study site is located at the Danube River, in Vienna, Austria (Fig. 1). The Viennese drinking water supply relies partially on water from the Danube River. The Danube River starts in Germany, approx. 850 km upstream, and shows dynamic variations in river discharge, ranging from 900 to 5300 m^3/s for the characteristic low and high discharges, with a mean discharge of 1900 m^3/s at the study site. The region has a temperate climate where floods are driven by snow melts and heavy rainfall events in the headwater catchment. The Danube River is moderately polluted with faecal matter that originates predominantly from human wastewater (Frick et al., 2017; Kirschner et al., 2017). The catchment upstream of Vienna is home to approx. 11 million inhabitants (Schreiber et al., 2005). Considering that 99% of the human population in the study area is connected to a WWTP (European Commission, 2018), urban wastewater is the main source of human pollution. This site is therefore representative of a large river polluted by upstream discharges of urban wastewater.

2.2. Modelling approach

Two models are applied in this study (Fig. 2). A hydrological model is used to simulate the river discharge in the Danube for a reference period (2003–2017) and a future period (2035–2049) based on regional climate model outputs (Parajka et al., 2016). The hydrological model domain encompasses the entire Danube subcatchment drained by the Danube up to the study site (104,000 km^2). A newly adapted version of the microbial fate and transport and infection risk model QMRAcatch is used to simulate the concentrations of viruses in river water at the study site and the required reduction of human viruses in source water to achieve safe drinking water (log reduction value, LRV). Its model domain is the 190-km-long Danube River section directly upstream of the study site and includes all sources of human wastewater, represented by: i) the effluent of five WWTPs situated 20, 24, 43, 77, and 193 km upstream of the study site and ii) the corresponding CSOs.

2.3. Hydrological model

To simulate the daily river flow rates of the Danube at the study site, we used a conceptual spatially-distributed hydrological model (Blöschl et al., 2008), which we extended for operational river flow forecasting. The structure is similar to that of the HBV model (Bergström, 1976) but several modifications were made including an additional groundwater storage, a bypass flow (Blöschl et al., 2008; Komma et al., 2008), and a modified routing routine. For each raster cell (5 km × 5 km), snow processes, soil moisture processes, and hill slope scale routing are simulated at an hourly time step. In the snow routine, snow accumulation and melt are represented by a simple degree-day concept. Runoff generation and changes in soil moisture storage are calculated by a soil moisture accounting scheme as a nonlinear function of rainfall and evaporation. Runoff is generated as a combination of outflows from three reservoirs representing overland flow, interflow, and deep groundwater flow processes. Runoff routing in the stream network is described by a cascade of linear reservoirs (Szolgay, 2004). More details and application examples are given, e.g., in Blöschl et al. (2008), Komma et al. (2008), and Reszler et al. (2008).

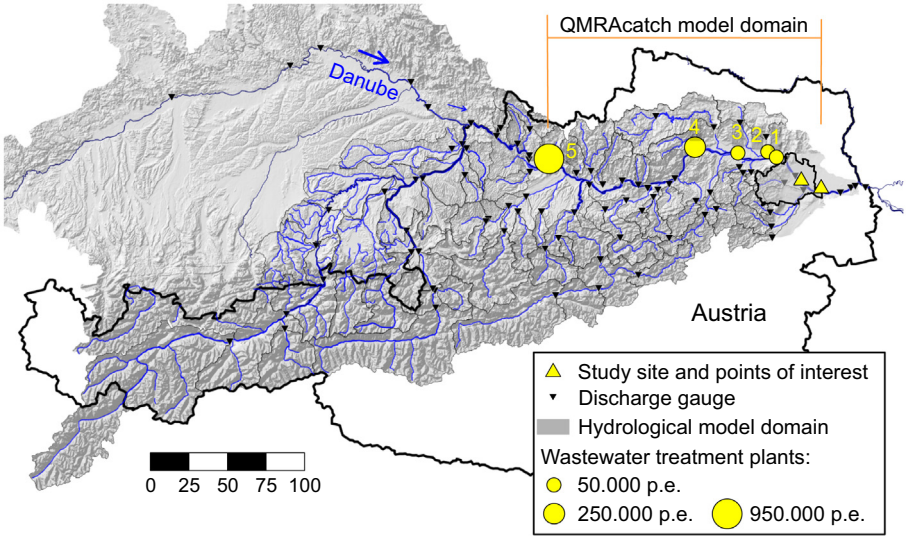

Fig. 1. Map of the study area.

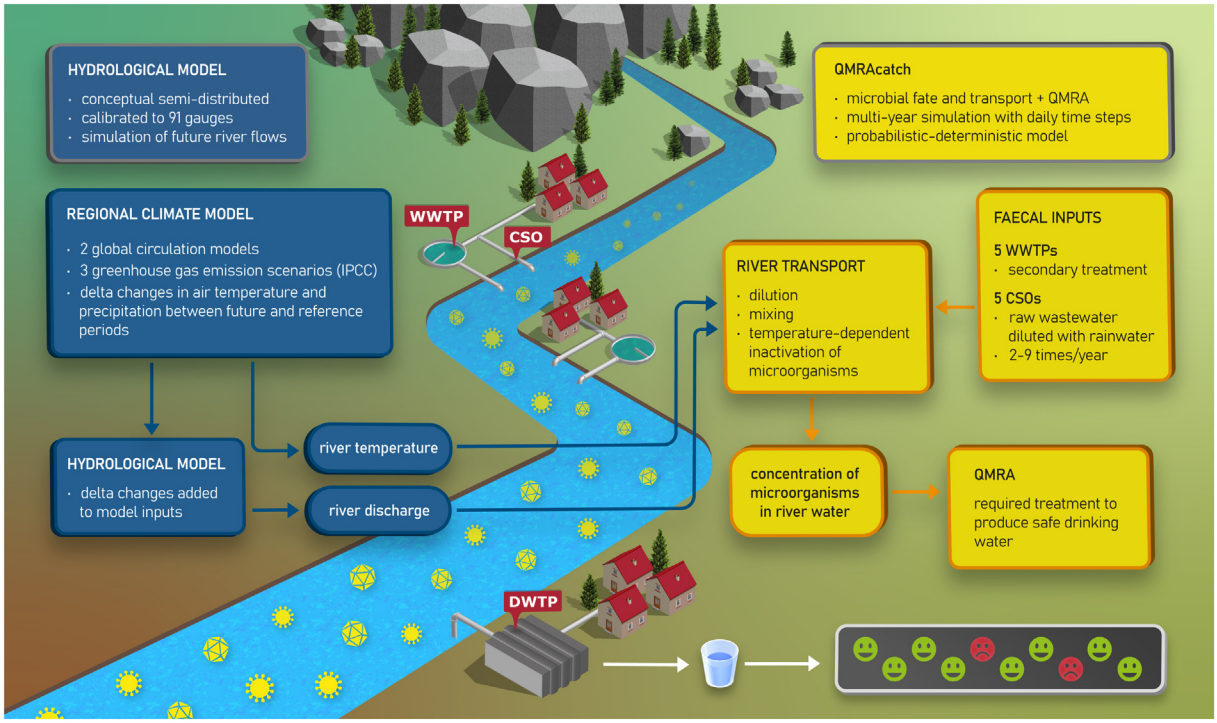

Fig. 2. Overview of model components.

In the extended version, the model input consists of spatially distributed fields of precipitation, air temperature, and potential evaporation. Meteorological and hydrological data were available for the period from 2003 to 2017 (provided by ZAMG and HZB, the central services for meteorology and hydrology in Austria). The data set includes several extreme flow periods, such as the 200-year flood in 2013 or the drought in 2015. The existence of hydro-meteorological extremes in the data set helps to estimate more robust and appropriate model parameters for predictions and extrapolation to future scenarios. For parameter identification, a hydrologic response unit approach based on spatial information about land use, soils, hydrogeology, and topography combined with a manual calibration procedure (Reszler et al., 2008) has been adopted. In this study, 15 different hydrologic response unit types were used to describe the different hydrological response behaviours (Table S1). The parameters have been calibrated and validated against hourly discharge data at 91 discharge gauges at the Danube and its tributaries. The simulation period included a calibration (2012 to 2018) and a validation period (2003 to 2011). The Nash and Sutcliffe coefficient of runoff model efficiency (Nash and Sutcliffe, 1970) at the 91 discharge gauges ranged between 0.72 and 0.84 for the calibration and between 0.66 and 0.85 for the validation period. The model efficiency for the calibration and validation period at the Danube gauge was 0.78 and 0.73, respectively.

2.4. QMRAcatch

2.4.1. Model overview

The probabilistic-deterministic microbial fate and transport and infection risk model QMRAcatch (Schijven et al., 2015) was extended for this study and newly coded as open source (v1.0 Python). QMRAcatch was used to estimate the microbial concentrations (Section 2.4.2) and the required reduction of reference pathogens to produce safe drinking water at the study site (Section 2.4.3). The model comprises the functionality of the original Mathematica version *QMRAcatch06062019.cdf* with the following extensions:

- Simulation time over multiple years in contrast to one year in the previous version.
- All model calculations are repeated for 100 to 1000 Monte Carlo simulations until results remain stable, to account for the natural variability and uncertainty of the model input parameters listed in Tables 1 and 3. In the previous version random values of all stochastic input variables were generated only once for each day in the simulation period.
- Pathogen loads are calculated from the simulated concentrations in river water at the study site.
- One CSO is located at each WWTP, as previously. The CSO discharge volumes and frequencies are now set independently from the continuous WWTP discharges. The days when CSOs occur are set to the days of observed rainfalls (during model calibration and validation) or randomly over the year based on a uniform probability distribution for each Monte Carlo run (scenario and sensitivity analysis).
- The transverse spreading of a continuous point source in a wide river flow was accounted for according to Jirka et al. (2004).
- In contrast to the previous version, the temperature-dependent microbial inactivation coefficients (for which site-specific values are not available) were set during model calibration within constrained limits based on reported persistence data.

2.4.2. Microbial fate and transport module

2.4.2.1. Faecal inputs. In QMRAcatch, the microbial concentration entering the WWTP (C_{raw}) is multiplied by the fraction of pathogens passing the WWTP ($Log_{10}\ F_{wwtp}$) to determine the concentration discharged to the surface water (C_{wwtp}). It is assumed that microbes in water samples at low concentrations are Poisson distributed. In Bayesian inference, the conjugate prior for the rate parameter of the Poisson distribution is the Gamma distribution. C_{raw} is therefore described by a gamma distribution (Table 1 for norovirus and enterovirus, Table S3 for *Cryptosporidium* and *Campylobacter*). The lognormal distribution was used here to describe the treatment efficiency of water (F_{WWTP}). It is convenient in that it describes the skewness of the treatment efficiency well and it is

Table 1
Model input parameters for norovirus and enterovirus (see Table S3 for Cryptosporidium and Campylobacter, as well as Table 3 for the parameters varied in the scenario analysis). Gamma probability distribution function (mean, 95th percentile) of the microbial concentrations in raw wastewater (C_{raw}), normal probability distribution function (mean, 95th percentile) of microbial removal by wastewater treatment (F_{WWTP}), WWTP effluent discharge rate (Q_{WWTP}), inactivation rate coefficients (a_0, a_1), and dose-response parameters α and β.

Parameter	Unit	Distribution	Details	Microorganism	Value	Reference
C_{raw} (mean, 95th perc.)	N/L	Gamma	WWTP 1,2,4,5 WWTP 3	Human MST marker	$(1.84, 5.82) \times 10^9$ $(1.04, 3.52) \times 10^9$	Schijven et al. (2015)
				Enterovirus	$(1.0, 2.0) \times 10^3$	(WHO, 2017b)
				Norovirus	$(1.0, 2.0) \times 10^5$	Katayama et al. (2008) Lodder and Husman (2005)
F_{WWTP} (mean, 95th perc.)	Log_{10}	Normal	WWTP 1,2,4,5 WWTP 3	Human MST marker	2.63, 2.15 2.25, 1.39	Derx et al. (2016)
				Enterovirus	1.8, 0.2	This study (calibrated)
				Norovirus	1, 0.75	Lodder and Husman (2005)
Q_{WWTP}	m^3/s	n.a.	WWTP1 to 5	–	0.30, 0.34, 0.17, 0.67, 7.24	Data provided by the EPA Austria
a_0, a_1	–	n.a.	First order decay in function of water temperature	Human MST marker	0.6, −0.035	This study (calibrated)
				Enterovirus	0.68, −0.036	This study (calibrated)
				Norovirus	2.3, −0.035	Bertrand et al. (2012) (mean value)
α, β	–	n.a.	Dose-response relationship: hypergeometric with beta-distributed parameters	Enterovirus	0.253, 0.422	Teunis et al. (1996)
				Norovirus	0.04, 0.055	Teunis et al. (2008)

easy to interpret. We generated random values for each Monte Carlo run by drawing from these distributions to reflect the temporal concentration variability. A constant discharge of treated wastewater (Q_{WWTP}) was attributed to WWTPs 1–5 based on previous annual discharge measurements at WWTPs 1–5 and in the rest of the QMRAcatch model domain (Fig. 1). The WWTPs provide secondary (conventional biological) treatment without chlorination or other tertiary treatment.

During CSO events, untreated wastewater mixed with rainwater discharges into the river. The microbial concentration in CSO water (C_{CSO}) is therefore a fraction of C_{raw}. The yearly CSO volumes were roughly estimated by Thomas Ertl and Florian Kretschmer (personal communication, Clara et al., 2014) based on the mean annual precipitation, the contributing runoff areas, the proportion of the combined sewer system, and the theoretical fraction of water piped to the WWTPs (ÖWAV, 2007).

2.4.2.2. Dilution in river water. The influx of microorganisms to the river water, through either a WWTP or a CSO, is diluted in river water. The mixing happens gradually as the water flows downstream. To calculate the cross-sectional concentration in the surface waters at X meters downstream of the emission, the transverse spreading of a continuous point source in a wide river flow (W >> h) was accounted for according to Jirka et al. (2004). The distance L_{mh} to the location where complete horizontal mixing over the river cross-section takes place was calculated by

$$L_{mh} = 0.4\frac{UW^2}{E_y} \quad (1)$$

where U is the flow velocity [m/s] calculated according to Manning (1891) and W is the river width [m] (Table A.1). The horizontal diffusivity E_y is calculated according to Fischer et al. (1979).

$$E_y = \alpha_y u^* h \quad (2)$$

where α_y is the diffusivity constant with a possible range of 0.5 ± 0.25 [−] for rivers without strong meanders and lateral dead zones, u^* is the friction velocity [m/s] and h is the river depth [m] (Table A.1). Vertical mixing was computed to be complete after a few hundred meters. The dilutions of microbial loads with river water are then calculated as

$$C_{river} = \sum_{i=1}^{n_{WWTP}} \left[\frac{\left(C_{WWTP_i} Q_{WWTP_i} + C_{CSO_i} Q_{CSO_i}\right)}{Q_{river}} \frac{L_{mh}}{X_i} \right] \quad (3)$$

where Q_{WWTPi} [m^3/s] is the discharge of treated wastewater at $WWTP_i$, Q_{CSOi} [m^3/s] is the CSO discharge, Q_{river} [m^3/s] is the river discharge, X_i is the distance of the point of interest to the pollution source [m], and n_{WWTP} is the number of WWTPs.

2.4.2.3. Inactivation during transport. The degree of removal of pathogens during transport depends on the travel time or flow rate. Inactivation during transport is described as a first order decay reaction, where the decay rate in water (μ_w [d^{-1}]) during transport is a function of the water temperature (T [°C]):

$$\mu_w(t) = \frac{ln\,10}{10^{a_0 + a_1 T}} \quad (4)$$

where a_0 [log_{10} day] and a_1 [log_{10} day °C^{-1}] are microorganism and pathogen-specific inactivation rate parameters (Bertrand et al., 2012). After a travel time of *m* days to the study site, microorganism concentrations ($C_{m,T}$ [m^{-3}]) are calculated as:

$$C_{m,T} = C_0\, exp\left(-\sum_{i=1}^{m} \mu_{W_i}\right) \quad (5)$$

where C_0 is the initial concentration [m^{-3}] and T_i is the temperature [°C] on the i^{th} day. The parameters a_0 and a_1 were determined using linear regression between reported times to first log_{10} reduction (TFL) versus water temperature. Inactivation rates that were reported in the literature were reviewed and summarized in Fig. B.1 and Table S2.

2.4.3. QMRA module

Daily probabilities of infection for enterovirus and norovirus can be estimated using a hypergeometric dose-response relation (Teunis and Havelaar, 2000):

$$P_{inf} = 1 - {}_1F_1(\alpha, \alpha + \beta, D) \quad (6)$$

$$D = C_{RW} \times 10^{LRV} \times I \times V \quad (7)$$

where P_{inf} is the daily probability of infection for a person per exposure, α, β are the parameters of dose-response models (Table 1), D is the dose of ingested microorganisms, C_{RW} is the microorganisms' concentration in the river water, LRV is the required treatment reduction of viruses, I is the infectious fraction, and V is the consumed unboiled water volume (1 L/person/day (WHO, 2017b)). As the daily health-based target (hbt), $1 \cdot 10^{-6}$ infections/person/day was adopted in this study (Signor and Ashbolt, 2009). LRV was estimated iteratively until the criterion $P_{inf} \leq$ hbt according to Eq. (6) was fulfilled for both the mean (μ) and 95th percentile values of P_{inf}.

$$LRV = \max\left[log_{10}\left(\frac{\mu^{P_{inf}}}{hbt}\right), log_{10}\left(\frac{95\%^{P_{inf}}}{hbt}\right)\right] \quad (8)$$

The dose-response model parameters for enterovirus were based on results from a human challenge study conducted with rotavirus where the minimum infectious dose for enterovirus was 1 focus forming unit (Ward et al., 1986). We used enterovirus data based on a cell culture method, detecting infectious enterovirus. The fraction of infectious to total viral particles is unknown for norovirus, as their enumeration method is based on PCR methods. However, the frequent occurrence of these viruses in outbreaks suggests high infectivity (Teunis et al., 2008). As the same authors pointed out, the resulting risk estimates might still be unbiased if the ratio of total to infectious numbers of viruses is constant because the exposure estimates in our scenarios are based on the same enumeration methods as in the human challenge study.

2.4.4. Microbial characterization of wastewater and river water

2.4.4.1. Microbiological analyses of wastewater. Values for C_{raw} and C_{wwtp} of the human-associated MST marker at WWTP2 and 3 were available from single 1-L samples collected from 2010 to 2013 (n=72, Schijven et al., 2015, Table 1). Additionally, values for C_{wwtp} of enterovirus at WWTP2 were isolated from 1-L samples between 2011 and 2017 (n=73) according to the inorganic flocculation and ultracentrifugation method of Walter and Rüdiger (1981) and enumerated following an MPN method (Chang et al., 1958) on Buffalo green monkey kidney cells (Dahling and Wright, 1986). For the concentrations of microorganisms in wastewater, QMRAcatch estimates the parameters of a Gamma distribution based on mean and 95th percentile values. The enterovirus concentrations were MPN values, i.e., maximum likelihood estimates, assuming Poisson distributed count observations. Given that these are concentration estimates already, concentration estimates of zero could be included in the calculation of the mean and 95th percentile values. We assumed a mean and 95th percentile of 1×10^3 and 2×10^3 MPN/L for C_{raw} of enterovirus, respectively (WHO, 2017b). F_{wwtp} was adjusted until the mean and 95th percentile of generated random values of C_{wwtp} matched the respective observed values (Table 1). Mean C_{raw} and F_{wwtp} values of 1×10^5 gene copies (gc)/L and 1-$\log_{10}$ for norovirus were assumed, respectively, according to Katayama et al. (2008) and Lodder and Husman (2005) (Table 1). The microbiological input parameters for *Cryptosporidium* and *Campylobacter* are described in Section 2 of the Supplementary information.

2.4.4.2. Microbiological analyses of river water. Surface water samples were collected from the Danube riverbank as grab samples at two sampling points (Fig. 1) alternately on a monthly basis over four years, resulting in a bi-weekly dataset of independent values (2013–2017, n=87–94). Because of the vicinity of the two points, they were treated as one point of interest for drinking water production, called hereafter 'the study site' (Fig. 1). The samples were analysed for the human-associated MST marker HF183/BacR287 as well as for infectious enterovirus. The human-associated MST marker was quantified in 500–600-mL water samples using quantitative PCR as described previously (Green et al., 2014; Mayer et al., 2018). The human-associated MST marker was detected in all samples with a median concentration of 1.1×10^4 ME/L (marker equivalent per litre) and a range of 4.0×10^2 to 1.4×10^6 ME/L (n=87, Fig. B.2). The filtration volume, the use of 2.5-μL of undiluted DNA extract in qPCR, and the minimal theoretically detectable marker concentration per reaction defines the detection threshold (3.0×10^2 ME/L) (Reischer et al., 2008). Infectious enteroviruses were enumerated from 10-L water samples according to the method described above. Enteroviruses were detected in 42% of the samples with a maximum concentration of 11.3 CU-MPN/L (cytopathic unit, most probable number, n=94). The limit of detection was 0.1 CU-MPN/L.

2.4.5. Calibration, validation, and application of QMRAcatch

Due to the limited availability of pathogen data in river water, we took a three-step approach for the calibration, validation and application of QMRAcatch: (1) model calibration and validation using the source-specific and highly abundant human-associated MST marker by adjusting the calibration parameters; (2) model calibration and validation using the reference pathogen enterovirus by adjusting just the microorganism- and virus-specific calibration parameters (the others taken over from step one); and (3) application of the calibrated and validated model to various pathogens (enterovirus, norovirus, *Campylobacter* and *Cryptosporidium*) by using measured data or values assumed from the literature as model inputs (overview in Table B.1, data in Tables 1 and S3).

The datasets of observed concentrations of the human-associated MST marker and enterovirus (n=87 and 94, respectively) were split into two time periods. Data for the period from July 2013 to June 2015 was used for calibration, and for the period from July 2015 to June 2017 for validation, for both microorganisms (Table B.1). Non-detects were set to the limit of detection in the calculations.

The mean absolute error (MAE) was used as a performance metric (Willmott and Matsuura, 2005). $\log_{10}$ transformed concentrations were used in the MAE computations because microorganisms typically follow a lognormal distribution, and the use of logarithms minimizes the influence of outliers present in the data (Hong et al., 2018). The Mann-Whitney test was used for the distribution comparisons of the simulated and observed datasets and the p-value of the Mann-Whitney statistic was a metric of model performance. During model calibration, the calibration parameters were adjusted to minimize the objective function (OF).

$$OF = MAE + (1-p) \quad (9)$$

The calibration parameters can be grouped into (i) not faecal microorganism and pathogen-specific and (ii) faecal microorganism and pathogen-specific parameters. The parameters of the first group describe the discharge and mixing processes which are assumed to be the same for faecal indicators and pathogens in river water. These are the constant diffusion coefficient α_y (Table A.1, Eqs. (1) and (2)), the frequency and discharge volumes of CSOs 1–5, and the microbial concentration in CSO water as a fraction of the concentration in raw wastewater (Table 3). The parameters of the second group are the microorganism- and virus-specific inactivation parameters a_0 and a_1 (Table 1). In the first step (calibration with the human-associated MST marker), calibration parameters of both groups were adjusted, and the best combination used for the validation. In the second step (calibration with enterovirus), the calibrated values of the parameters of the first group were taken over from step 1 and kept constant, and only the parameters of the second group were adjusted. The best combination of the calibration parameter settings was used for the validation. The CSO volumes per year were constrained to ±25% of the yearly estimates (Section 2.4.2). The CSO events were constrained to days when the daily amount of rainfall exceeded 13 mm/d. Recorded precipitation data were used at gauges Vienna Hohe Warte (at WWTPs 1 and 2), Langenlebarn (at WWTP 3), Krems (at WWTP 4), and Linz-City (at WWTP 5, data provided by the Austrian Meteorology Survey, ZAMG). Inactivation rates of the human-associated MST marker, enterovirus, and norovirus that were reported in the literature were collected and summarized in Fig. B.1 and Table S2. Boehm et al. (2019) conducted an extensive literature review on inactivation studies for viruses and conducted a multiple linear regression analysis between environmental variables and first-order decay rates. Enterovirus inactivation rates showed a statistically significant relationship with temperature, method and sunlight, therefore we restricted our selection to studies conducted with cell

culture (so that they are comparable to our results, see Section 2.4.4) and in natural or artificial sunlight. The coefficient 'water type' was not significant in the multiple linear regression, therefore we included all water types (marine and estuarine – no study was conducted in freshwater in sunlight). Norovirus only showed a significant relationship with temperature so we included all studies listed by Boehm et al. (2019) (Table S2). An ordinary least square method was used to fit the time-to-first-log (TFL) as a function of water temperature (dashed lines in Fig. B.1). During the adjustment of intercept a_0 and slope a_1 (used in Eq. (4), solid lines in Fig. B.1), it was ensured that the inactivation as function of temperature obtained through the calibration lay within the prediction interval of the ordinary least square regressions (Fig. B.1, shaded area, left and centre).

2.5. Scenario analysis

We defined a reference scenario and the following future scenarios: i) climate and demographic changes and ii) three scenarios of wastewater management measures that aim to reduce the faecal load from WWTPs and CSOs. Table 2 provides an overview of the scenarios. Additionally, we conducted a sensitivity analysis to investigate the impact of CSO changes. For all scenarios and the sensitivity analysis, the concentrations of enterovirus, norovirus, *Cryptosporidium* and *Campylobacter* in the Danube were simulated using the input settings as described in Tables 1, 3 and S3. Subsequently, a QMRA was conducted for assessing the required LRV to achieve the health-based target.

2.5.1. Reference scenario

We simulated the concentrations of norovirus and enterovirus in river water at the study site, as well as the required LRVs to produce safe drinking water for the reference period from 2003 to 2017. This period included hydrologically extreme years and was therefore deemed a robust basis for the scenario analysis (Tables 2 and 3).

2.5.2. Future scenarios

2.5.2.1. Climate and demographic changes: 'No management changes' scenario. In this study, flow projections of future climate scenarios were modelled using a hydrological model forcing from a delta change approach as described in detail by Parajka et al. (2016). In a first step, regional climate model (RCM) outputs were used to estimate monthly differences in air temperature and precipitation between reference (control) and future periods (2035–2049). These differences (delta changes) were then added to the observed precipitation and air temperature data and used as model inputs to simulate future hydrologic changes (Fig. C.1). The daily precipitation was scaled by the relative delta changes for each month, and the frequency of rainy days was kept as in the reference period. The daily air temperature was changed by the mean daily delta changes each month. To obtain future delta changes in water temperature, the delta changes of daily air temperature were multiplied by seasonal conversion factors derived from the observed changes in air and water temperatures of the Danube from 1900 to 2010 (Standhartinger and Godina, 2013, p. 46, Fig. 11). The conversion factors for December, January, and February resulted in 1.22; for March, April, and May they resulted in 0.52; for June, July, and August they resulted in 0.76; and for September, October, and November they resulted in 1.5.

The RCM scenarios used in this study are based on the results of the reclip:century project (Loibl et al., 2011; Parajka et al., 2016). The ensemble climate projections are represented by COSMO-CLM RCM runs forced by the ECHAM5 and HADCM3 global circulation models for three different Intergovernmental Panel on Climate Change (IPCC) emission scenarios (A1B, B1, and A2; Nakicenovic et al., 2000). These represent a large spread of different emission pathways based on no change in greenhouse gas emission practices (A2), a scenario with a moderate decline in emissions after 2050 (A1B), and a scenario indicating considerably reduced emissions from the present onwards (B1). For this study, the projections by the ECHAM5 model were selected for the three emission scenarios (A1B, A2, B1), as well as the projections by the HADCM3 model for one emission scenario (A1B). Although these scenarios are meanwhile replaced by the Representative Concentration Pathways (RCPs, van Vuuren et al. (2011)) these older scenarios are still comparable to the newer RCPs with respect to their climate change signals. Moreover, the model setup for RCM simulations of reclip:century are specifically tailored for the complex terrain of the Alpine Region and therefore provide more robust estimates of the future climate change in the Alps and surrounding areas (Blöschl et al., 2018; Blöschl et al., 2017).

The reclip:century scenarios project, for the study area, changes in air temperature and precipitation between the future period 2035–2049 and the reference period 2003–2017. Precipitation projections show that winters will become 5% (HADCM3 A1B) to 22% (ECHAM5 A2) wetter and extreme precipitation quantities will increase. Predictions of future precipitation changes for summer range from 4% (HADCM3 A1B) to −21% (ECHAM5 A2). These changes are generally in line with the newer generation of RCM simulation from the EURO-CORDEX initiative where an ensemble of simulations for RCP4.5 and 8.5 are downscaled for the Austrian domain. Only the EURO-CORDEX ensemble mean summer precipitation change signal for Austria is +3% for RCP8.5, showing somewhat different results compared to ECHAM5 A2, however, the ensemble spread in EURO-CORDEX is rather large pointing towards higher uncertainties during the summer season.

For the study site of the Danube, all climate scenarios project a general decrease of river flows during the low flow period (summer) and a slight increase or no change of river flow during the high flow period (end of winter/spring). The river flow in the Danube study catchment is expected to decrease on average by 14% (ECHAM5 A1B) to 25% (ECHAM5 A2), with a slight increase of about 10%–15% in January and February for the ECHAM5 A1B scenario and an almost 50% decrease in August for the ECHAM5 A2 scenario (Fig. C.1).

Population growth will result in a corresponding increase in urban wastewater discharges into the Danube. An increase in wastewater discharge volumes by 14% until 2050 was considered at WWTPs 1–5, according to the projected population growth of Lower Austria, the state covering the majority of the model domain (Austria, 2017, Tables 2 and 3).

2.5.2.2. Scenarios of wastewater management measures

2.5.2.2.1. 'Enhanced wastewater treatment' scenario. The current EU regulations for WWTPs require a reduction of organic carbon, nitrogen,

Table 2
Overview of the scenario analysis. +: taken into account, −: not applicable/not applied.

Scenario	Climate change (river discharge and temperature)	Population growth (WWTP discharge)	Enhanced wastewater treatment	CSO prevention
Reference	−	−	−	−
No management changes	+	+	−	−
CSO prevention	+	+	−	+
Enhanced wastewater treatment	+	+	+	−
CSO prevention and enhanced wastewater treatment	+	+	+	+

Table 3
Model input parameters for the reference scenario (2003–2017) and future scenarios (2035–2049) as well as for the sensitivity analysis, for the study site in the Danube.

Parameter	Dimension	Reference scenario	Description of future change	Future scenarios/sensitivity analysis
Population growth and climate change				
Effluent discharge at WWTPs 1–5	m^3/s	See Table 1	Population growth	+14% (Austria, 2017)
Daily river discharge at study site	m^3/s	Hydrological modelling for period 2003–2017	Climate scenarios ECHAM5-A1B, A2, B1, HADCM3-A1B (Loibl et al., 2011, Parajka et al., 2016) (Section 2.5.2.1)	Hydrological modelling from 2035 to 2049
Daily river water temperature	°C	Data records at Danube gauge Greifenstein from 2003 to 2018 (viadonau, 2019)		Delta changes in air temperature and season-specific conversion factors (Section 2.5.2.1)
Changes due to wastewater management measures				
Log_{10} reduction by wastewater treatment (F_{wwtp})	Log_{10}	See Table 1	Additional treatment	+ 4 (Campos et al., 2016, Francy et al., 2012, Gerrity et al., 2012, Owens et al., 2000, Paraskeva and Graham, 2002)
CSO frequency	N/year	At WWTP 1: 2 At WWTP 2: 2.5 At WWTP 3: 9.5 At WWTP 4: 5.5 At WWTP 5: 4 (calibrated)	Complete prevention of CSOs through, e.g., reservoirs	0
CSO discharge at WWTPs 1–5	m^3/s	At WWTP 1: 0.89 At WWTP 2: 1.01 At WWTP 3: 0.52 At WWTP 4: 2.00 At WWTP 5: 21.73 (calibrated)	Complete prevention of CSOs through, e.g., reservoirs	0
Sensitivity to changes in CSOs				
CSO frequency at WWTPs 1–5	N/year	Calibrated (see above)	More frequent extreme rainfall events	Up to 3-fold increase
CSO discharge at WWTPs 1–5	m^3/year	Calibrated (see above)	More frequent extreme rainfall events	Up to 3-fold increase
Concentration of pathogens in CSO water	–	0.1 (calibrated)	Fraction of the concentration in raw wastewater	0.1 and 1.0 (de Man et al., 2014, Sterk et al., 2016)

and phosphorous, but there are no microbiological requirements or obligations for disinfection (European Commission, 1998). A possible strategy to reduce the load of pathogens from WWTPs is to include ozonation and/or UV irradiation as tertiary wastewater treatment. According to previous reports, the efficiency of disinfection during wastewater treatment on reducing virus concentrations can remarkably vary, depending on the dose of chemicals or the UV fluence, from 1.5 to 4 log_{10} particles/L by ozonation (Gerrity et al., 2012; Owens et al., 2000; Paraskeva and Graham, 2002) or UV irradiation (Campos et al., 2016; Francy et al., 2012). We considered an additional treatment step at at WWTPs 1–5 that reaches a reduction of entero- and norovirus by 4 log_{10} in the scenarios (Tables 2 and 3).

2.5.2.2.2. 'CSO prevention' scenario. A further possible measure is to prevent CSO events using, for example, stormwater reservoirs, retention basins, rain barrels, green roofs, permeable patios, or grassed swales (Demuzere et al., 2014; Lewellyn et al., 2016; Pazwash, 2016). We assumed that the measures are capable of completely preventing CSOs (Tables 2 and 3).

2.5.2.2.3. 'CSO prevention and enhanced wastewater treatment' scenario. A combination of the above two wastewater management measures was considered in the fourth future scenario.

2.5.3. Sensitivity analysis to investigate the effects of increased storm events

The extreme storm event frequency is thought to increase with warming at a rate similar to the water vapour holding capacity of the air, the so-called Clausius-Clapeyron rate, at ~7%/°C (Molnar et al., 2015). CSOs are therefore likely to happen more frequently, but their reaction to changes in rainfall is highly non-linear (Willems et al., 2012). Considering this high uncertainty, we did not include an increased rate or intensity of CSOs in the future scenarios (they were kept the same as in the reference scenario) but conducted a sensitivity analysis to investigate how changes in CSO discharge volumes and frequencies would modulate the future scenarios. We took the 'no management changes' and 'enhanced wastewater treatment' scenarios as baselines. The above-listed two variables were varied individually, while the settings for all other parameters were kept the same as those for the baselines (Table 3).

3. Results

3.1. Model calibration and validation

The QMRAcatch model was calibrated and validated in two consecutive steps: First, against data on the human-associated MST marker and second, against data on enterovirus measured at the study site (Table B.1). From the calibration parameters, the model proved to be the most sensitive to the microorganism and virus-specific inactivation rate parameters a_0 and a_1 during the manual calibration. The parameters were constrained so that the resulting time to first log reduction versus water temperature function remained within the 95% prediction interval of the regression line fit to experimental values for both microorganisms (Fig. B.1, Tables 1 and S2).

The Mann-Whitney tests indicated that the simulated and observed concentrations were not significantly different for the human-associated MST marker and enterovirus ($p>0.05$, Table 4). The cumulative distribution plot of the simulated and observed concentrations is shown in Fig. B.2.

The model errors within the 5-95th percentiles ranged from −1.3 to 1.3 log_{10} N/L for the human-associated MST marker and from −1.1 to 1.5 log_{10} N/L for enterovirus (Figs. B.2 and B.3). The error distributions were very similar for the calibration and validation periods. The OF values were almost the same in the validation period as in the calibration period for the human-associated MST marker. The OF values for

Table 4
Model performance for simulated microbial concentrations at the study site after 1000 Monte Carlo runs.

	Parameter	Time period	n (n of detects)	Mann-Whitney test, p-value	Mean absolute error [log_{10} (N/L)]	Objective function (Eq. (9))
Calibration	Human MST marker	2013–2015	44 (44)	0.61	0.54	0.9
	Enterovirus	2013–2015	46 (17)	0.75	0.62	0.9
Validation	Human MST marker	2015–2017	43 (43)	0.59	0.63	1.0
	Enterovirus	2015–2017	48 (22)	0.13	0.64	1.5

enterovirus were the same as for the human-associated MST marker for the calibration period, but slightly higher for the validation period.

3.2. Scenario analysis: virus concentration and required LRV

QMRAcatch was applied to simulate the reference and four future scenarios using the calibrated settings but with river flows and temperatures as simulated by the regional climate and hydrological models (Fig. 2, Tables 2 and 3). For these scenarios, we simulated pathogen concentrations in river water at the study site and calculated the required treatment reduction (LRV) of pathogens from river water for the production of safe drinking water. The viral reference pathogens norovirus and enterovirus were the primary focus of the analysis. For cross-comparisons, the scenario analysis was additionally performed for *Cryptosporidium* and *Campylobacter* (results reported in Section 2 of the Supplementary information).

3.2.1. Reference

For the reference period, the median and range of concentrations of enterovirus at the study site were −0.55 (−2.84 to 2.54) log_{10} N/L, while they were 3 orders of magnitude higher for norovirus: 2.30 (1.23 to 3.23) log_{10} N/L (Fig. 3, top, Table C.1). The required LRV was 6.3 and 8.4 log_{10} for enterovirus and norovirus, respectively (Fig. 3, bottom).

3.2.2. Future climate, population, and no management changes

Four regional climate scenarios were tested, covering the entire range of expected climate pathways. They showed similar results in terms of the simulated concentrations of enterovirus and norovirus in river water as well as the LRVs (Fig. C.2, Table C.1). The climate scenario ECHAM5 A2, based on no efforts taken to reduce greenhouse gas emissions, was chosen as the basis for all future scenarios. Based on this climate scenario, the discharge of the Danube River at the study site will be up to 50% lower during low flows (summer-autumn), while only

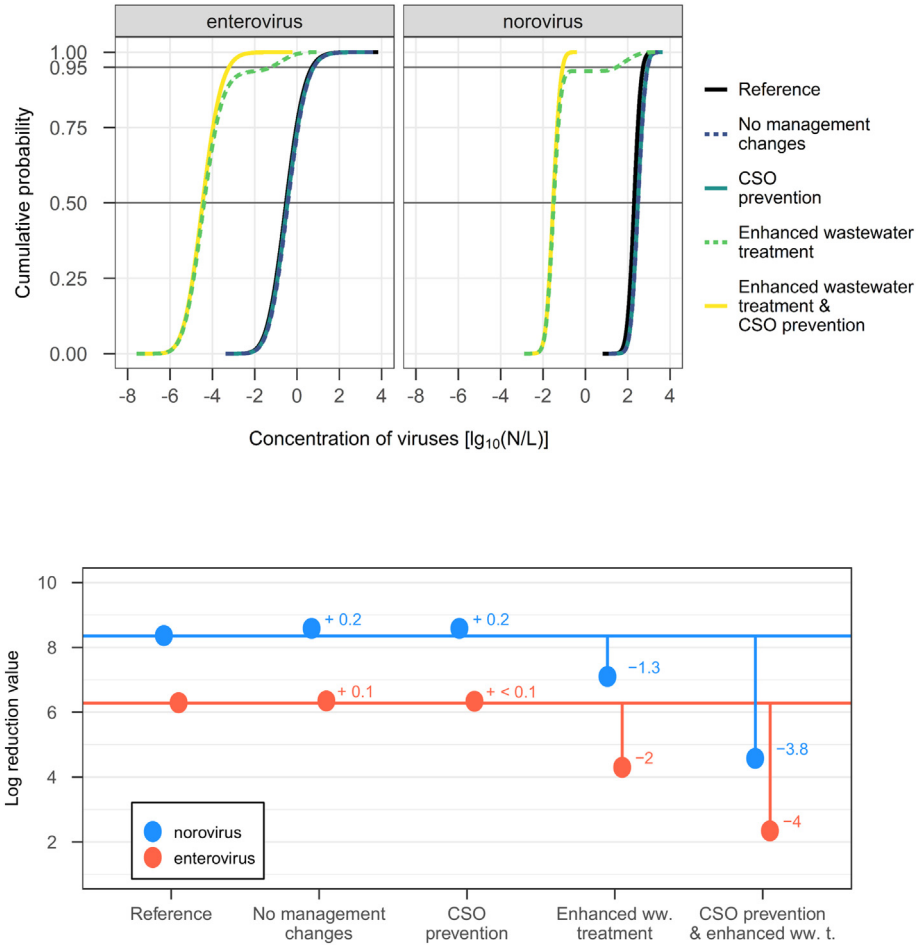

Fig. 3. Scenario simulations for norovirus and enterovirus (see Fig. S1 for the results for Cryptosporidium and Campylobacter). Upper panel: Simulated concentrations in river water. The 'CSO prevention' scenario entirely overlaps with the 'no management changes' one. Bottom panel: Required virus log reduction values to achieve safe drinking water.

slightly higher during high flows (late winter-spring). The temperature of river water will be 2 °C higher on average (Figs. C.1 and C.3).

In comparison to the reference period, the projected climatic and demographic changes showed a negligible effect on the concentrations of enterovirus and norovirus in river water as well as on the required LRVs (Fig. 3, Table C.1).

3.2.3. Future climate, population, and prevention of CSOs

While preventing CSO events precluded a few peaks of virus concentration in the river, it did not affect the overall distribution of concentrations, which remained similar to the reference and 'no management changes' scenarios (Fig. 3, top, Table C.1). The LRVs were not affected either (Fig. 3, bottom).

3.2.4. Future climate, population, and enhanced wastewater treatment

The installation of a tertiary treatment step at the five WWTPs (assumed effect: 4 $\log_{10}$) reduced the median concentrations of enterovirus and norovirus in river water by 3.9 and 3.8 $\log_{10}$, respectively, compared to the reference scenario. However, the maximum concentrations were only slightly reduced (1.9 and 0.1 $\log_{10}$ lower), and a batch of virus concentration peaks 3 to 5 $\log_{10}$ higher than the median remained (Fig. 3, top and Table C.1). The LRVs for enterovirus and norovirus were 2.0 and 1.3 $\log_{10}$ lower than in the reference scenario (Fig. 3, bottom).

3.2.5. Future climate, population, and combination of enhanced wastewater treatment and prevention of CSOs

The measure reduced both the median and maximum virus concentrations at the study site by approximately 4 $\log_{10}$ compared to the reference scenario (Fig. 3, top, Table C.1). The LRVs were 3.9 and 3.8 $\log_{10}$ lower than in the reference scenario (Fig. 3, bottom).

The observed pattern of the scenario analysis was found to be principally the same for all four reference pathogens (Fig. 3 for norovirus and enterovirus, Fig. S1 for *Campylobacter* and *Cryptosporidium*).

3.3. Sensitivity of future scenarios to uncertainties in CSO predictions

Considering the lack of information regarding the effect of climate change on CSOs, we conducted a sensitivity analysis to see how changes in CSOs would modulate the two future scenarios with CSO events ('no management changes' and 'enhanced wastewater treatment'). We varied two factors: the frequency of CSO events and the volume of CSO events (up to a 3-fold increase compared to the reference). We calculated the LRVs for enterovirus and norovirus.

In the 'no management changes' scenario, varying the frequency and the volume of CSO events had no or very little effect on the LRVs. In contrast, in the 'enhanced wastewater treatment' scenario, the same variations in the frequency and volume of CSO events had a considerable effect on the LRVs. An increase in the frequency of CSOs had a more pronounced effect on the LRVs, with 0.35 to 0.40 $\log_{10}$ higher LRVs for a 100% increase in CSO frequency, compared to 0.23 $\log_{10}$ higher LRVs for a 100% increase in CSO volumes (Fig. 4).

The above results show that the 'no management changes' scenario is not sensitive to an increase in CSOs. However, in the 'enhanced wastewater treatment' scenario, the required LRV for enterovirus and norovirus could be up to 1.03 and 0.74 $\log_{10}$ higher, respectively, depending on how the frequency and volumes of CSOs are affected by climate change (Fig. 4).

Additionally, we assessed the effect of the virus concentration in CSO water on the LRV. In the two baseline scenarios, the virus concentration in CSO water is assumed to be 10% of that of raw wastewater. Increasing it to equal raw wastewater did not cause changes in the predictions for the 'no management changes' case; however, it increased the LRV values by 1 $\log_{10}$ for the 'enhanced wastewater treatment' case (results not shown).

3.4. Scenario analysis: source apportionment of the load of viruses at the study site

The above results of the scenario analysis raise some intriguing questions about the effect of the wastewater management measures targeting WWTPs and/or CSOs (Section 3.2) and their interplay with climate and population changes (Section 3.3). To better understand this effect, we conducted a source apportionment of the load of pathogens at the study site originating from WWTPs and from CSOs. We did this by running each scenario twice: once by setting all pathogen inputs from WWTPs to zero and once by setting all inputs from CSOs to zero. We then calculated the daily load of pathogens at the study site by multiplying the simulated daily concentrations at the study site by the daily river flows. Fig. 5 displays the sum of loads from WWTPs and CSOs, i.e., the entire load of viruses in each scenario together with the percentage contribution of WWTPs and CSOs (Fig. S2 shows the same for *Cryptosporidium* and *Campylobacter*).

The analysis revealed that under the current situation and in the 'no management changes' scenario, WWTPs discharging secondary treated wastewater were the major contributors to the load of viruses at the study site (10^{10} N/d enterovirus and 10^{13} N/d norovirus, 97–99% of the total load). The rest, 1–3%, originated from CSOs that discharge

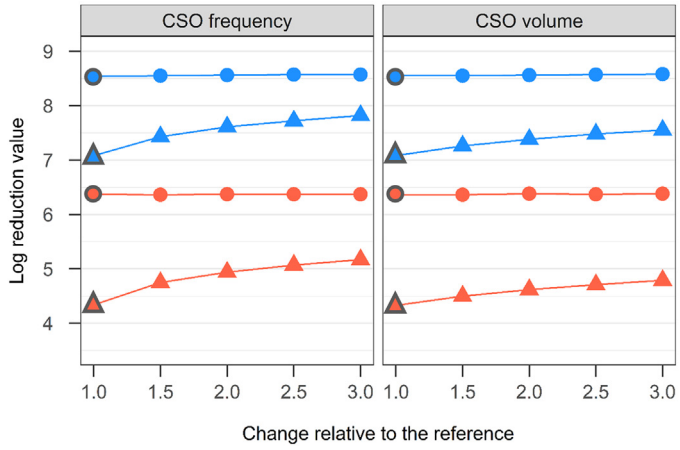

Legend and regressions

Virus	Enhanced treatment	CSO frequency: Slope (sign.)	CSO frequency: Std. error of slope	CSO frequency: R^2	CSO volume: Slope (sign.)	CSO volume: Std. error of slope	CSO volume: R^2
norovirus	0	0.02 (**)	<0.01	0.94	0.02 (**)	<0.01	0.94
	4	0.35 (**)	0.06	0.92	0.23 (**)	0.02	0.97
enterovirus	0	<0.01 (n.s.)	<0.01	0.13	0.01 (n.s.)	<0.01	0.63
	4	0.40 (**)	0.07	0.91	0.23 (**)	0.02	0.97

Fig. 4. Effect of various future CSO changes on the required log reduction value (LRV). The black contour shows the 'no management changes' (circle) and 'enhanced wastewater treatment' (triangle) scenarios. The table shows the results of linear regression analyses for enhanced treatment achieving an additional reduction of viruses of 0 or 4 $\log_{10}$; n.s., not significant; **, $p < 0.01$.

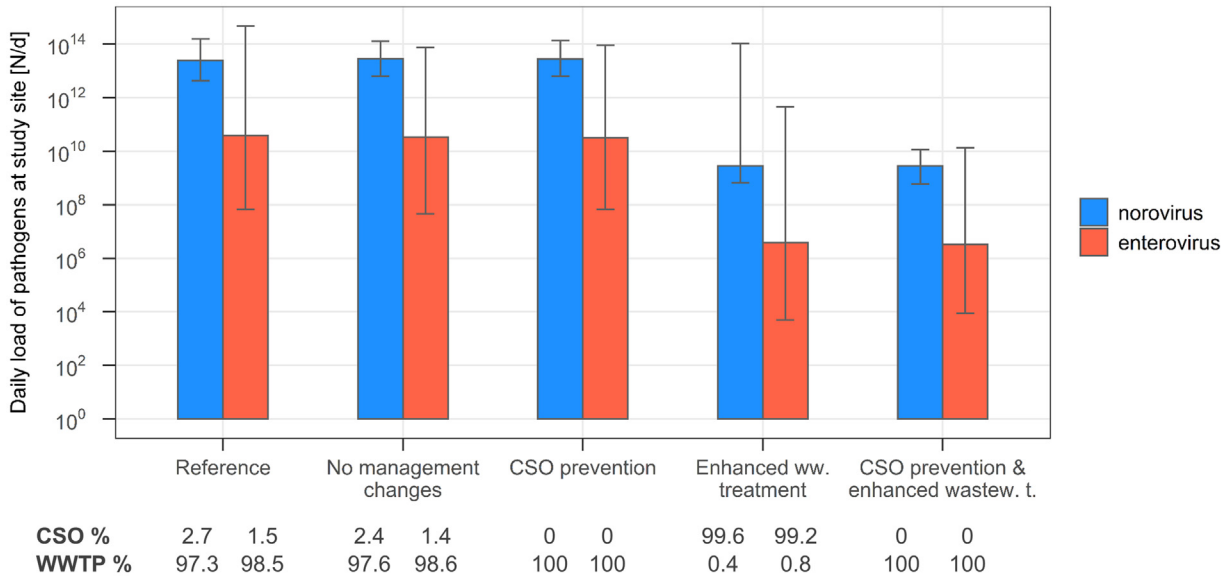

Fig. 5. Scenarios: Median daily load of norovirus and enterovirus at the study site and relative source apportionment. The whiskers show the range of simulated daily loads. See Fig. S2 for the results for *Cryptosporidium* and *Campylobacter*.

raw wastewater diluted with rainwater (Fig. 5). This explains why changes in CSOs (neither their prevention nor their increase due to climate change) did not affect virus concentration distributions and LRVs (Figs. 3 and 4). It also explains why enhanced wastewater treatment was effective at improving river microbial water quality (LRVs reduced by 1.3 and 2 $\log_{10}$, for norovirus and enterovirus, Fig. 3): It addressed the main contributor to the pollution load.

This source contribution relationship between WWTPs and CSOs flipped once enhanced wastewater treatment was in place: the main contributors were then the CSOs, with 10^6 N/d enterovirus and 10^9 N/d norovirus contributing over 99% to the total load. The median daily load was reduced by 4 $\log_{10}$; however, the maximum daily loads were reduced by only 0.2 and 3.1 $\log_{10}$ for norovirus and enterovirus, respectively (Fig. 5). This means a highly unequal distribution of the pollution load over time: While on days with no CSO events the daily load is relatively low, showing the beneficial effect of enhanced wastewater treatment, on days with CSOs the load is up to 5 $\log_{10}$ higher. The same pattern is visible in the virus concentration results (Fig. 3, top). Also, this predominance of CSOs explains why a climate-change-driven increase in CSOs affects LRVs so remarkably if enhanced wastewater treatment is in place (Fig. 4), and why the prevention of CSOs ('CSO prevention and enhanced wastewater treatment ' scenario) resulted in such a pronounced additional decrease of LRVs (an additional 2.5 and 1.9 $\log_{10}$ reduction of viruses, Fig. 3, bottom).

This pattern observed at the viral reference pathogens proved to be similar in the case of the bacterial and protozoan reference pathogens (*Campylobacter* and *Cryptosporidium*, Fig. S2).

4. Discussion

In this study, we tested an integrative modelling approach that combines CO_2 emission scenarios of the IPCC, a regional climate model, a conceptual hydrological model of the catchment as well as the significantly extended version of the microbial fate, transport and infection risk model QMRAcatch. The latter was used to estimate the source apportionment and the pathogen concentration in river water for QMRA. The combination of these methodological aspects was the key in gaining insights into the effects of future climatic and demographic changes and their interplay with possible upgrades in wastewater infrastructure on the microbiological water quality of rivers.

4.1. Implications of the assumptions and uncertainties of the modelling approach

Here, we discuss the model assumptions in this study, the uncertainty in the choice of input parameters, and their implications on the results. To assess the effects of climate change, monthly differences of air temperature and precipitation between simulations for a reference (2003–2017) and a future period (2035–2049) were calculated based on regional climate model outputs and used as input to a hydrological model. To investigate the changes in intense rainfall events and the impact on CSOs, however, methods that account for the spatial and temporal variability of rainfall would be needed (Muller-Thomy et al., 2018). Hydraulic modelling of the sewer system, e.g., by using the urban stormwater model SWMM, would enable the studying of these effects on CSOs. For example, Bi et al. (2015) found a 15–500% increase in the volume discharged by CSOs in 2050 as compared to 2013 in Canada. This highlights that the relationship between changes in precipitation and CSO variables is not linear. How the contaminant concentration in CSO water will change in the future is also very much specific to the urban area and the sewer system drained by the CSO. An in-depth and location-specific analysis of urban sewer systems and their response to climate change was beyond the focus of this study.

As a wastewater upgrade for WWTPs, we assumed that enhanced treatment achieves an additional 4-log reduction of enterovirus and norovirus concentrations. While we added this value to the mean and 95th percentile of the assumed normal probability distribution of secondary treatment, a more realistic approach would be to apply distributions of microorganism- and process-specific values. The concentration of pathogens in WWTP effluent was assumed to be the same in the future as it is now. However, there may be differences in the disease burden in the future (Levy et al., 2016).

Our study focuses on two pathogenic human viruses, enterovirus and norovirus, and their source, human wastewater. As an extension, we compare these results with a bacterial and a protozoan reference pathogen, *Campylobacter* and *Cryptosporidium*. Since these latter two may basically also originate from reservoirs other than humans, it is important to note that the current study focussed on the human-wastewater-associated fraction of these pathogens for direct cross-comparisons to the viral refence pathogens, assuming human communal waste water as the dominating pollution source.

The above-listed uncertainties and assumptions affect the absolute LRVs to achieve safe drinking water for all scenarios likewise. We aimed to study the effects of various changes of the system on microbiological drinking water safety requirements, not absolute LRV values.

4.2. Accurateness of the pathogen fate and transport predictions

In order to accurately predict the reference pathogen concentrations and loads, the model calibration and validation of the fate and transport model based on site- and source-specific data are seen as an essential step. To evaluate QMRAcatch, we used measured MST and enterovirus concentrations collected at the study site over four years.

Our literature survey on reported MST marker and virus inactivation rates revealed a current lack of studies conducted in real-world and natural light conditions, in particular for norovirus, which creates a source of model uncertainty. In order to overcome this limitation, we set the microbial inactivation coefficients during calibration within constrained limits based on reported persistence data for the human-associated MST marker and enterovirus.

The use of human-associated MST data allowed for source-targeted calibration and validation of the model (Mayer et al., 2018; Zhang et al., 2019). The human-associated MST marker thus provides a better basis for calibration and validation in the context of our research questions (on point sources of human wastewater) than a standard faecal indicator organism, such as *E. coli* would do, since *E. coli* may, for example, also originate from other non-faecal sources (Frick et al., 2018). Integrating pathogen data in the calibration-validation process is an essential confirmation, and it allows to assess health risks directly (Boehm and Soller, 2013; Lodder et al., 2015). However, pathogens can hardly serve as the basis for a comprehensive calibration on their own, since their concentrations in environmental waters are often very low, and the required large sample volumes and processing efforts render the establishment of large data series unfeasible. Still, a smaller pathogen dataset may complement the calibration process. The human-associated MST marker has approx. 4–6 $\log_{10}$ higher concentrations in raw wastewater than most pathogens, and often maintains high concentrations in environmental waters. Therefore, the model calibration followed a nested approach to make optimal use of both the host-associated MST marker and pathogen data. Discharge and mixing processes of faecal pollution associated microorganisms and pathogens in river water could be robustly calibrated using sufficiently abundant source-targeted MST marker data. The pathogen data were then used to adjust the model to the pathogen-specific inactivation rate coefficients. The calibrated and validated model was then able to simulate the low, non-detectable but significant ranges of the enteric pathogens in question or even simulate new pathogens, where only information on the concentrations in sewage and environmental persistence is available (Table B.1). Despite the advantages of this systematic approach, only a few microbial fate and transport modelling studies have used it so far (Derx et al., 2016; Schijven et al., 2015).

4.3. Deciphering the interplay of future changes and wastewater management measures

Several studies investigated the effects of future changes in climate, population or wastewater infrastructure on the microbiological river water quality so far, but the controlling factors remain yet unclear (Iqbal et al., 2019; Islam et al., 2018a; Jalliffier-Verne et al., 2017; Sterk et al., 2016). This study brought new insights into this question by integrating source apportionment, concentrations of reference pathogens and risk assessment into a modelling analysis. Source apportionment was previously used to identify the dominant sources of faecal indicator bacteria (Soller et al., 2014; Stapleton et al., 2011) or to study the effects of sociodemographic and climate changes on faecal indicator bacteria loads into a river (Iqbal et al., 2019). Our study identified source apportionment together with the other methodological aspects of the integrative modelling approach as the key for understanding for the first time the interplay of future changes and wastewater management measures. We showed how this interplay affects pathogen loads into rivers, and the pathogen concentrations in rivers considering safe drinking water production.

For the scenario with no management changes at our example study site, changes in river flows and water temperatures were shown to have a minor negative effect on the microbiological river water quality, in line with the predictions for other regions (Iqbal et al., 2019, Islam et al., 2018a, Jalliffier-Verne et al., 2017, Sterk et al., 2016). According to the reference scenario, WWTPs discharging secondary treated sewage are the major contributors to the pathogen loads, not CSOs. Therefore, neither potential increases in CSO events due to climate change nor their prevention affected the drinking water safety requirements. In contrast, if enhanced wastewater treatment was in place at the WWTPs, CSOs suddenly became the major contributors to the pathogen loads. Here, climate-change driven increases in CSO events resulted in significantly higher treatment requirements. While this issue was addressed earlier by Sterk et al. (2016) in the context of bathing water infection risks, our modelling results for the first time identify the conditions and extent to which increased CSOs affect the microbiological river water quality in the context of safe drinking water production.

The greatest improvement in the microbiological water quality of the riverine water intake was achieved with measures targeting both WWTPs and CSOs. The Austrian Waste and Wastewater Association estimates that an additional yearly investment of 150 million Euros is needed to tackle upcoming problems in this sector in the coming years (ÖWAV, 2020). Since the current regulatory standard is secondary treatment at the WWTPs, it is very important to evaluate the benefits enhanced wastewater treatment would bring, which is currently discussed in the context of micropollutant abatement. Furthermore, it is important to estimate the impact of urban soil sealing, an important yet often neglected aspect in city development, with respect to the microbiological water quality of the receiving waters.

5. Conclusions

- The pathogen fate and transport and infection risk model QMRAcatch (v1.0 Python) was significantly extended and is now available as open source.
- Climatic and demographic changes had little impact on the microbiological river water quality considering safe drinking water, where 98% of the pathogen loads stemmed from WWTP discharges. Strong climate change effects are shown in the scenario with enhanced WWTP treatment, where CSOs are the major faecal pollution sources.
- The required log reduction value (LRV) to produce safe drinking water was 6.3, 8.4, 4.9 and 5.1 $\log_{10}$ for enterovirus, norovirus, *Campylobacter* and *Cryptosporidium* in the scenario with secondary WWTP treatment. Enhanced wastewater treatment led to a reduction of LRVs by 0.5 to 2.0 $\log_{10}$. This measure combined with preventing CSOs had the most significant positive effect with a reduction of LRVs by up to 4 $\log_{10}$.
- The integrative modelling framework is demonstrated at a large, wastewater-impacted river, and is applicable at other catchments and types of pollution sources for long-term water safety planning.

Software availability

The source code for QMRAcatch v1.0 python is available upon request. The original Mathematica version is available at www.waterandhealth.at.

Funding sources

This work was supported by the Niederösterreichische Forschungs- und Bildungsgesellschaft (NFB) [grant number LSC 19-016 "Future Danube"], by the Austrian Science Fund (FWF) as part of the Vienna Doctoral Program on Water Resource Systems [grant number W1219], by the Vienna Science and Technology Fund (WWTF) [grant number ESR17-070] and by the European Union and Vienna Water [programme number LE07-13, project name 'Groundwater Resource Systems Vienna']. Vienna Water was involved in parts of the research. This is reflected by the authorship of an expert who is affiliated there. None of the other funding sources had an involvement in the study.

CRediT authorship contribution statement

Katalin Demeter: Data curation, Formal analysis, Investigation, Writing – original draft, Writing – review & editing, Visualization. **Julia Derx:** Methodology, Software, Formal analysis, Investigation, Writing – original draft, Writing – review & editing. **Jürgen Komma:** Formal analysis, Investigation, Writing – original draft. **Juraj Parajka:** Formal analysis, Investigation, Writing – original draft. **Jack Schijven:** Software, Writing – original draft. **Regina Sommer:** Conceptualization, Funding acquisition. **Silvia Cervero-Aragó:** Investigation, Writing – original draft. **Gerhard Lindner:** Investigation. **Christa M. Zoufal-Hruza:** Investigation, Writing – original draft. **Rita Linke:** Investigation, Writing – original draft. **Domenico Savio:** Investigation. **Simone K. Ixenmaier:** Investigation. **Alexander K.T. Kirschner:** Conceptualization, Funding acquisition. **Harald Kromp:** Conceptualization. **Alfred P. Blaschke:** Conceptualization, Funding acquisition, Supervision. **Andreas H. Farnleitner:** Conceptualization, Writing – original draft, Writing – review & editing, Funding acquisition, Supervision.

Declaration of competing interest

The authors declare that they have no known competing financial interests or personal relationships that could have appeared to influence the work reported in this paper.

Acknowledgements

We would like to thank the viadonau for providing the discharge and temperature data of the Danube River. We thank the EPA Austria (Umweltbundesamt) for providing data on the discharges at the WWTPs and Prof. Thomas Ertl and Florian Kretschmer for information on CSO volumes in selected Austrian cities. We thank Prof. Matthias Zessner for providing information regarding EU WWTP standards, and Alexander Chik for his consultation regarding our microbiological data analysis as well as Klaus Haslinger for his support with comparing the climate change predictions. We would also like to thank the three anonymous reviewers whose constructive comments greatly improved the manuscript. This is a joint investigation within the Interuniversity Cooperation Centre for Water & Health (www.waterandhealth.at).

Appendix A. QMRAcatch model details

Table A.1
River dimensions and intermediate calculations for dilution of microbial concentrations with river water.

River geometry			
W	Width of the river	250	[m]
h	Depth of the river	4	[m]
s	Slope of the river bed	0.0004	[−]
Constants			
n	Manning coefficient	0.024	[m $s^{-0.3}$]
α_y	Diffusivity constant, calibrated	0.35	[−]
g	Gravitation constant	9.81	[m s^{-2}]
Intermediate calculations			
R_h	Hydraulic radius	$=\frac{W \cdot h}{W+2h}$ =3.9	[m]
U	Average flow velocity (Manning, 1891)	$=\frac{R_h^{2/3}\sqrt{s}}{n}$=2.1	[m/s]
u^*	Friction velocity	$=\sqrt{g \cdot h \cdot s}$=0.1	[m/s]

Appendix B. Additional information to the calibration and validation

Table B.1
A tiered approach to the application of the model to various targeted microorganisms and pathogens. n.a.: not applied.

Microorganism/pathogen	QMRAcatch calibration	QMRAcatch validation	Scenario simulations
Human-associated MST marker	Yes Dataset 2013–2015	Yes Dataset 2015–2017	n.a.
Enterovirus	Yes Dataset 2013–2015	Yes Dataset 2015–2017	Yes, input data partially measured, partially from literature
Norovirus	n.a.	n.a.	Yes, input data from literature
Campylobacter	n.a.	n.a.	Yes, input data from literature
Cryptosporidium	n.a.	n.a.	Yes, input data measured

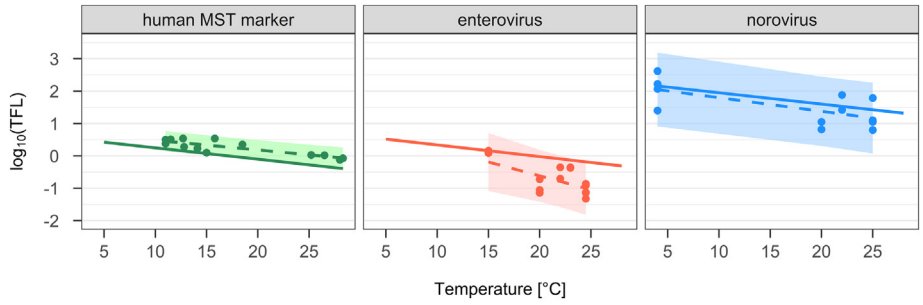

Fig. B.1. Inactivation of the human-associated MST marker, enterovirus, and norovirus as applied in this study (solid lines) and as reported in experimental studies (dots, Table S2), plotted as time to first $\log_{10}$ reduction (TFL, days) values $\log_{10}$-transformed ($\log_{10}$(TFL)) in function of the temperature. Ordinary-least-square regressions (dashed lines) were fitted to the literature values, shown with their 95% prediction intervals (shaded). The intercept and the slope of the solid lines were the result of the model calibration for the human MST marker and enterovirus, and are the reported values of Bertrand et al. (2012) for norovirus. These values were used as model input parameters a_0 and a_1 in Eq. (4) (Table 1).

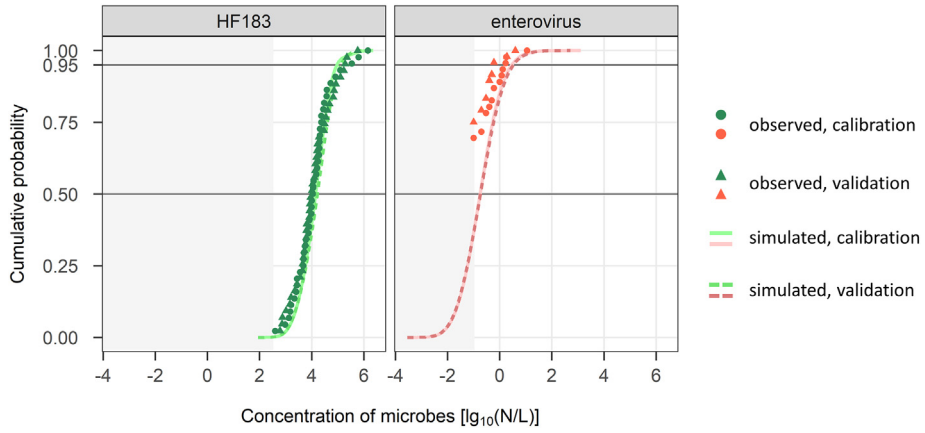

Fig. B.2. Simulated and observed concentrations of the human-associated MST marker and of enterovirus during calibration and validation. The light grey area marks values under the detection threshold for the human-associated MST marker (qPCR) and under the limit of detection for enterovirus (MPN method).

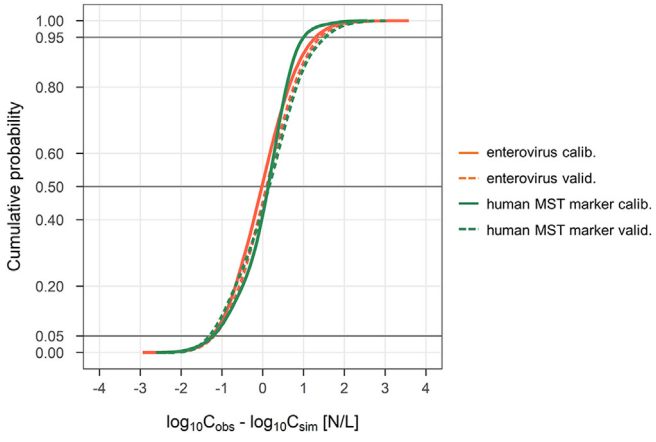

Fig. B.3. Calibration and verification. Cumulative distribution plot of the difference between the simulated and measured concentrations ($\log_{10}$-transformed) of the human-associated MST marker and enterovirus for the calibration and validation periods.

Appendix C. Additional information to the scenario analysis

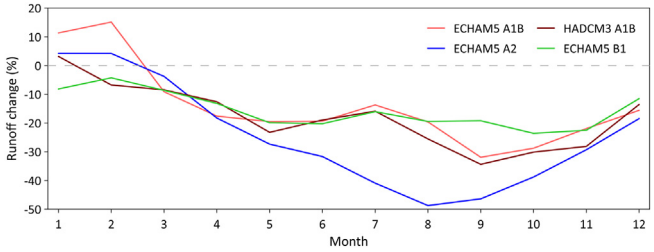

Fig. C.1. Mean monthly change of the river flow for the Danube River in Vienna, estimated according to four climate projections: ECHAM5 A1B, ECHAM5 A2, ECHAM5 B1 and HADCM3 A1B, where A1B, B1, and A2 represent three Intergovernmental Panel on Climate Change emission scenarios, and ECHAM 5 and HADCM3 are two global climate models. The change represents the relative change between the reference period 2003–2017 and the future period 2035–2049.

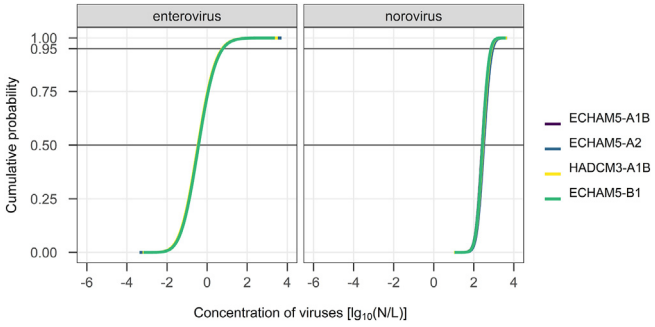

Fig. C.2. Simulated concentrations of norovirus and enterovirus in river water according to the four climate scenarios considered in this study.

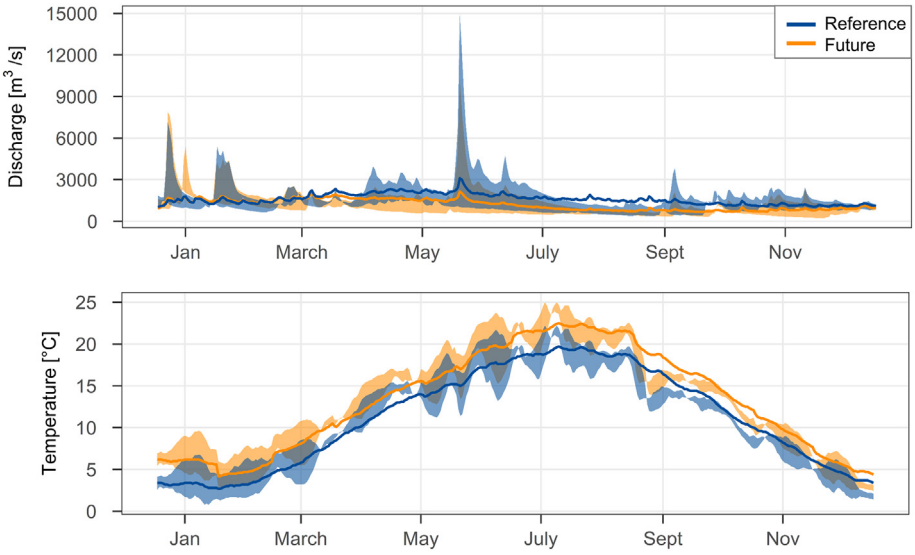

Fig. C.3. Discharge (upper panel) and water temperature (lower panel) of the Danube in the study area for the reference period (2003–2017) and the future period (2035–2049). The projections are based on the ECHAM5 A2 climate scenario. The line shows the mean across the 15 years, while the ribbon shows the range between the year with the lowest yearly mean discharge/temperature and the year with the highest one.

Table C.1
Simulated concentration of enterovirus and norovirus in river water at the study site in the scenario analysis. For each scenario, 100 Monte Carlo runs were simulated. Each statistic is given by the median and range across the 100 runs.

		Simulated concentration [$\log_{10}$(N/L)]		
Virus	Scenario	Median (range of median)	Min (range of min)	Max (range of max)
Scenarios of global change and wastewater infrastructure upgrades				
Enterovirus	Reference	−0.55 (−0.58 to −0.51)	−2.84 (−3.33 to −2.61)	2.54 (1.78 to 3.58)
	No management changes	−0.47 (−0.50 to −0.44)	−2.83 (−3.54 to −2.48)	2.59 (2.05 to 3.53)
	CSO prevention	−0.49 (−0.51 to −0.45)	−2.84 (−3.52 to −2.55)	2.61 (1.98 to 3.73)
	Enhanced ww. treatment	−4.43 (−4.45 to −4.40)	−6.84 (−7.53 to −6.51)	0.68 (0.44 to 1.25)
	Enhanced ww. treatment & CSO prevention	−4.49 (−4.51 to −4.46)	−6.86 (−7.32 to −6.59)	−1.45 (−2.10 to −0.61)
Norovirus	Reference	2.30 (2.29 to 2.31)	1.23 (0.81 to 1.46)	3.23 (3.07 to 3.50)
	No management changes	2.49 (2.48 to 2.50)	1.40 (1.10 to 1.57)	3.47 (3.34 to 3.66)
	CSO prevention	2.48 (2.47 to 2.49)	1.42 (1.11 to 1.56)	3.44 (3.30 to 3.65)
	Enhanced ww. treatment	−1.50 (−1.51 to −1.49)	−2.61 (−2.89 to −2.41)	3.15 (2.94 to 3.61)
	Enhanced ww. treatment & CSO prevention	−1.52 (−1.53 to −1.51)	−2.61 (−2.83 to −2.41)	−0.57 (−0.71 to −0.40)
Climate scenarios				
Enterovirus	ECHAM5-A1B	−0.44 (−0.47 to −0.42)	−2.74 (−3.31 to −2.47)	2.57 (2.08 to 3.46)
	ECHAM5-A2	−0.47 (−0.50 to −0.44)	−2.83 (−3.54 to −2.48)	2.59 (2.05 to 3.53)
	HADCM3-A1B	−0.45 (−0.47 to −0.42)	−2.75 (−3.22 to −2.44)	2.54 (2.08 to 3.53)
	ECHAM5-B1	−0.43 (−0.45 to −0.41)	−2.74 (−3.17 to −2.43)	2.62 (2.05 to 3.39)
Norovirus	ECHAM5-A1B	2.42 (2.41 to 2.43)	1.33 (1.06 to 1.54)	3.38 (3.26 to 3.65)
	ECHAM5-A2	2.49 (2.48 to 2.50)	1.40 (1.10 to 1.57)	3.47 (3.34 to 3.66)
	HADCM3-A1B	2.44 (2.44 to 2.45)	1.32 (1.01 to 1.55)	3.37 (3.25 to 3.66)
	ECHAM5-B1	2.43 (2.42 to 2.44)	1.34 (1.04 to 1.56)	3.34 (3.23 to 3.59)

Appendix D. Supplementary data

Supplementary data to this article providing more details on model calibration and validation as well as all results of the scenario simulations for *Cryptosporidium* and *Campylobacter* can be found online at https://doi.org/10.1016/j.scitotenv.2020.144278.

References

Austria, S., 2017. Population in Yearly Average From 1952 to 2100 (STATcube - Statistische Datenbank von STATISTIK AUSTRIA).

Bergström, S., 1976. Development and Application of a Conceptual Runoff Model for Scandinavian Catchments.

Bertrand, I., Schijven, J.F., Sanchez, G., Wyn-Jones, P., Ottoson, J., Morin, T., Muscillo, M., Verani, M., Nasser, A., Husman, A.M.D., Myrmel, M., Sellwood, J., Cook, N., Gantzer, C., 2012. The impact of temperature on the inactivation of enteric viruses in food and water: a review. J. Appl. Microbiol. 112 (6), 1059–1074.

Bi, E., Monette, F., Gachon, P., Gasperi, J., Perrodin, Y., 2015. Quantitative and qualitative assessment of the impact of climate change on a combined sewer overflow and its receiving water body. Environmental Science and Pollution Research International 22.

Blöschl, G., Reszler, C., Komma, J., 2008. A spatially distributed flash flood forecasting model. Environ. Model. Softw. 23 (4), 464–478.

Blöschl, G., Parajka, J., Blaschke, A.P., Hofstätter, M., Haslinger, K., Schöner, W., 2017. Klimawandel in der Wasserwirtschaft – Schwerpunkt Hochwasser, Dürre und Trockenheit, Follow up zur ZAMG/TU-WIEN STUDIE (2011) Anpassungsstrategien an den Klimawandel für Österreichs für Österreichs Wasserwirtschaft im Autrag von Bund und Ländern (Bundesministerium für Nachhaltigkeit und Tourismus).

Blöschl, G., Blaschke, A.P., Haslinger, K., Hofstätter, M., Parajka, J., Salinas, J., Schöner, W., 2018. Impact of climate change on Austria's water sector—an updated status report. Österreichische Wasser- und Abfallwirtschaft 70, 462–473.

Blöschl, G., Hall, J., Viglione, A., Perdigão, R.A.P., Parajka, J., Merz, B., Lun, D., Arheimer, B., Aronica, G.T., Bilibashi, A., Boháč, M., Bonacci, O., Borga, M., Čanjevac, I., Castellarin, A., Chirico, G.B., Claps, P., Frolova, N., Ganora, D., Gorbachova, L., Gül, A., Hannaford, J., Harrigan, S., Kireeva, M., Kiss, A., Kjeldsen, T.R., Kohnová, S., Koskela, J.J., Ledvinka, O., Macdonald, N., Mavrova-Guirguinova, M., Mediero, L., Merz, R., Molnar, P., Montanari, A., Murphy, C., Osuch, M., Ovcharuk, V., Radevski, I., Salinas, J.L., Sauquet, E., Šraj, M., Szolgay, J., Volpi, E., Wilson, D., Zaimi, K., Živković, N., 2019. Changing climate both increases and decreases European river floods. Nature 573 (7772), 108–111.

Boehm, A.B., Soller, J.A., 2013. Environmental Toxicology: Selected Entries From the Encyclopedia of Sustainability Science and Technology. Laws, E.A. (ed), pp. 441-459, Springer New York, New York, NY.

Boehm, A.B., Silverman, A.I., Schriewer, A., Goodwin, K., 2019. Systematic review and meta-analysis of decay rates of waterborne mammalian viruses and coliphages in surface waters. Water Res. 164, 13.

Campos, C.J.A., Avant, J., Lowther, J., Till, D., Lees, D.N., 2016. Human norovirus in untreated sewage and effluents from primary, secondary and tertiary treatment processes. Water Res. 103, 224–232.

Chang, S.L., Berg, G., Busch, K.A., Stevenson, R.E., Clarke, N.A., Kabler, P.W., 1958. Application of the most probable number method for estimating concentrations of animal viruses by the tissue culture technique. Virology 6 (1), 27–42.

Cho, K.H., Pachepsky, Y.A., Oliver, D.M., Muirhead, R.W., Park, Y., Quilliam, R.S., Shelton, D.R., 2016. Modeling fate and transport of fecally-derived microorganisms at the watershed scale: state of the science and future opportunities. Water Res. 100, 38–56.

Clara, M., Ertl, T., Giselbrecht, G., Gruber, G., Hofer, T.F., Humer, F., Kretschmer, F., Kolla, L., Scheffknecht, C., Weiß, S., Windhofer, G., 2014. SCHTURM - Spurenstoffemissionen aus Siedlungsgebieten und von Verkehrsflächen (Endbericht). Austria, Vienna.

Dahling, D.R., Wright, B.A., 1986. Optimization of the BGM cell line culture and viral assay procedures for monitoring viruses in the environment. Appl. Environ. Microbiol. 51 (4), 790–812.

de Man, H., van den Berg, H.H.J.L., Leenen, E.J.T.M., Schijven, J.F., Schets, F.M., van der Vliet, J.C., van Knapen, F., de Roda Husman, A.M., 2014. Quantitative assessment of infection risk from exposure to waterborne pathogens in urban floodwater. Water Res. 48, 90–99.

Demuzere, M., Orru, K., Heidrich, O., Olazabal, E., Geneletti, D., Orru, H., Bhave, A.G., Mittal, N., Feliu, E., Faehnle, M., 2014. Mitigating and adapting to climate change: multi-functional and multi-scale assessment of green urban infrastructure. J. Environ. Manag. 146, 107–115.

Derx, J., Blaschke, A.P., Farnleitner, A.H., Pang, L., Bloschl, G., Schijven, J.F., 2013. Effects of fluctuations in river water level on virus removal by bank filtration and aquifer passage - a scenario analysis. J. Contam. Hydrol. 147, 34–44.

Derx, J., Schijven, J., Sommer, R., Zoufal-Hruza, C.M., van Driezum, I.H., Reischer, G., Ixenmaier, S., Kirschner, A., Frick, C., de Roda Husman, A.M., Farnleitner, A.H., Blaschke, A.P., 2016. QMRAcatch: human-associated fecal pollution and infection risk modeling for a river/floodplain environment. J. Environ. Qual. 45 (4), 1205–1214.

Dorner, S.M., Anderson, W.B., Slawson, R.M., Kouwen, N., Huck, P.M., 2006. Hydrologic modeling of pathogen fate and transport. Environ. Sci. Technol. 40 (15), 4746–4753.

Eregno, F.E., Tryland, I., Tjomsland, T., Myrmel, M., Robertson, L., Heistad, A., 2016. Quantitative microbial risk assessment combined with hydrodynamic modelling to estimate the public health risk associated with bathing after rainfall events. Sci. Total Environ. 548-549, 270–279.

European Commission (1998) Commission Directive 98/15/EC of 27 February 1998 amending Council Directive 91/271/EEC of 21 May 1991 concerning urban waste-water treatment with respect to certain requirements established in Annex I thereof (Text with EEA relevance).

European Commission (2018) Urban waste water website: Austria. http://uwwtd.oieau.fr/Austria/ Accessed on 25th January 2018.

Fauvel, B., Gantzer, C., Cauchie, H.M., Ogorzaly, L., 2017. In situ dynamics of F-specific RNA bacteriophages in a small river: new way to assess viral propagation in water quality studies. Food and Environmental Virology 9 (1), 89–102.

Fischer, H.B., List, E.J., Koh, R.C.Y., Imberger, J., Brooks, N.H., 1979. Mixing in Inland and Coastal Waters. Academic Press, San Diego.

Francy, D.S., Stelzer, E.A., Bushon, R.N., Brady, A.M.G., Williston, A.G., Riddell, K.R., Borchardt, M.A., Spencer, S.K., Gellner, T.M., 2012. Comparative effectiveness of membrane bioreactors, conventional secondary treatment, and chlorine and UV disinfection to remove microorganisms from municipal wastewaters. Water Res. 46 (13), 4164–4178.

Frick, C., Zoufal, W., Zoufal-Hruza, C., Kirschner, A.K.T., Seidl, D., Derx, J., Sommer, R., Blaschke, A.P., Nadiotis-Tsaka, T., Farnleitner, A.H., 2017. The microbiological water quality of Vienna's River Danube section and its associated water bodies. Österreichische Wasser- und Abfallwirtschaft 69 (1-2), 76–88. https://doi.org/10.1007/s00506-016-0349-9.

Frick, C., Vierheilig, J., Linke, R., Savio, D., Zornig, H., Antensteiner, R., Baumgartner, C., Bucher, C., Blaschke, A.P., Derx, J., Kirschner, A.K.T., Ryzinska-Paier, G., Mayer, R., Seidl, D., Nadiotis-Tsaka, T., Sommer, R., Farnleitner, A.H., 2018. Poikilothermic animals as a previously unrecognized source of fecal indicator bacteria in a backwater ecosystem of a large river. Appl Environ Microbiol 84(16), aem.00715-00718.

Gerrity, D., Gamage, S., Jones, D., Korshin, G.V., Lee, Y., Pisarenko, A., Trenholm, R.A., von Gunten, U., Wert, E.C., Snyder, S.A., 2012. Development of surrogate correlation models to predict trace organic contaminant oxidation and microbial inactivation during ozonation. Water Res. 46 (19), 6257–6272.

Golden, H.E., Hoghooghi, N., 2018. Green infrastructure and its catchment-scale effects: an emerging science. Wiley Interdisciplinary Reviews-Water 5 (1).

Green, H.C., Haugland, R.A., Varma, M., Millen, H.T., Borchardt, M.A., Field, K.G., Walters, W.A., Knight, R., Sivaganesan, M., Kelty, C.A., Shanks, O.C., 2014. Improved HF183 quantitative real-time PCR assay for characterization of human fecal pollution in ambient surface water samples. Appl. Environ. Microbiol. 80 (10), 3086–3094.

Hong, E.M., Park, Y., Muirhead, R., Jeong, J., Pachepsky, Y.A., 2018. Development and evaluation of the bacterial fate and transport module for the Agricultural Policy/Environmental eXtender (APEX) model. Sci. Total Environ. 615, 47–58.

Iqbal, M.S., Islam, M.M.M., Hofstra, N., 2019. The impact of socio-economic development and climate change on E-coli loads and concentrations in Kabul River, Pakistan. Sci. Total Environ. 650, 1935–1943.

Islam, M.M.M., Iqbal, M.S., Leemans, R., Hofstra, N., 2018a. Modelling the impact of future socio-economic and climate change scenarios on river microbial water quality. Int. J. Hyg. Environ. Health 221 (2), 283–292.

Islam, M.M.M., Sokolova, E., Hofstra, N., 2018b. Modelling of river faecal indicator bacteria dynamics as a basis for faecal contamination reduction. J. Hydrol. 563, 1000–1008.

Jalliffier-Verne, I., Leconte, R., Huaringa-Alvarez, U., Madoux-Humery, A.S., Galarneau, M., Servais, P., Prévost, M., Dorner, S., 2015. Impacts of global change on the concentrations and dilution of combined sewer overflows in a drinking water source. Sci. Total Environ. 508, 462–476.

Jalliffier-Verne, I., Leconte, R., Huaringa-Alvarez, U., Heniche, M., Madoux-Humery, A.S., Autixier, L., Galarneau, M., Servais, P., Prévost, M., Dorner, S., 2017. Modelling the impacts of global change on concentrations of Escherichia coli in an urban river. Adv. Water Resour. 108, 450–460.

Jirka, G.H., Bleninger, T., Burrows, R., Larsen, T., 2004. Environmental quality standards in the EC-water framework directive: consequences for water pollution control for point sources. Eur. Water Manag. Online 1–20.

Katayama, H., Haramoto, E., Oguma, K., Yamashita, H., Tajima, A., Nakajima, H., Ohgaki, S., 2008. One-year monthly quantitative survey of noroviruses, enteroviruses, and adenoviruses in wastewater collected from six plants in Japan. Water Res. 42 (6–7), 1441–1448.

Kim, M., Boithias, L., Cho, K.H., Silvera, N., Thammahacksa, C., Latsachack, K., Rochelle-Newall, E., Sengtaheuanghoung, O., Pierret, A., Pachepsky, Y.A., Ribolzi, O., 2017. Hydrological modeling of fecal indicator bacteria in a tropical mountain catchment. Water Res. 119, 102–113.

Kirschner, A.K.T., Reischer, G.H., Jakwerth, S., Savio, D., Ixenmaier, S., Toth, E., Sommer, R., Mach, R.L., Linke, R., Eiler, A., Kolarevic, S., Farnleitner, A.H., 2017. Multiparametric monitoring of microbial faecal pollution reveals the dominance of human contamination along the whole Danube River. Water Res. 124, 543–555.

Komma, J., Blöschl, G., Reszler, C., 2008. Soil moisture updating by Ensemble Kalman Filtering in real-time flood forecasting. J. Hydrol. 228–242.

Levy, K., Woster, A.P., Goldstein, R.S., Carlton, E.J., 2016. Untangling the impacts of climate change on waterborne diseases: a systematic review of relationships between diarrheal diseases and temperature, rainfall, flooding, and drought. Environmental Science & Technology 50 (10), 4905–4922.

Lewellyn, C., Lyons, C.E., Traver, R.G., Wadzuk, B.M., 2016. Evaluation of seasonal and large storm runoff volume capture of an infiltration green infrastructure system. J. Hydrol. Eng. 21 (1).

Lodder, W.J., Husman, A.M.D., 2005. Presence of noroviruses and other enteric viruses in sewage and surface waters in The Netherlands. Appl. Environ. Microbiol. 71 (3), 1453–1461.

Lodder, W.J., Schijven, J.F., Rutjes, S.A., Husman, A.M.D., Teunis, P.F.M., 2015. Entero- and parechovirus distributions in surface water and probabilities of exposure to these viruses during water recreation. Water Res. 75, 25–32.

Loibl, W., Formayer, H., Schöner, W., Truhetz, H., Anders, I., Gobiet, A., Heinrich, G., Köstl, M., Nadeem, I., Peters Anders, J., Schicker, I., Suklitsch, M., Züger, H., 2011. reclip:century 1 Research for Climate Protection: Century Climate Simulations: Models, Data and GHG Scenarios, Simulations. ACRP final Report Reclip: Century Part A, Vienna, 22.

Manning, R., 1891. On the flow of water in open channels and pipes. Transaction of the Institution of Civil Engineers of Ireland 20, 161–207.

Mayer, R.E., Reischer, G.H., Ixenmaier, S.K., Derx, J., Blaschke, A.P., Ebdon, J.E., Linke, R., Egle, L., Ahmed, W., Blanch, A.R., Byamukama, D., Savill, M., Mushi, D., Cristobal, H.A., Edge, T.A., Schade, M.A., Aslan, A., Brooks, Y.M., Sommer, R., Masago, Y., Sato, M.I., Taylor, H.D., Rose, J.B., Wuertz, S., Shanks, O.C., Piringer, H., Mach, R.L., Savio, D., Zessner, M., Farnleitner, A.H., 2018. Global distribution of human-associated fecal genetic markers in reference samples from six continents. Environ Sci Technol 52 (9), 5076–5084.

Medema, G.J., Schijven, J.F., 2001. Modelling the sewage discharge and dispersion of cryptosporidium and giardia in surface water. Water Res. 35 (18), 4307–4316.

Molnar, P., Fatichi, S., Gaal, L., Szolgay, J., Burlando, P., 2015. Storm type effects on super Clausius-Clapeyron scaling of intense rainstorm properties with air temperature. Hydrol. Earth Syst. Sci. 19 (4), 1753–1766.

Muller-Thomy, H., Wallner, M., Forster, K., 2018. Rainfall disaggregation for hydrological modeling: is there a need for spatial consistence? Hydrol. Earth Syst. Sci. 22 (10), 5259–5280.

Myhre, G., Alterskjær, K., Stjern, C.W., Hodnebrog, Ø., Marelle, L., Samset, B.H., Sillmann, J., Schaller, N., Fischer, E., Schulz, M., Stohl, A., 2019. Frequency of extreme precipitation increases extensively with event rareness under global warming. Sci. Rep. 9 (1), 16063.

Nakicenovic, N., Alcamo, J., Davis, G., de Vries, B., Fenhann, J., Gaffin, S., Gregory, K., Grübler, A., Jung, T.Y., Kram, T., La Rovere, E.L., Michaelis, L., Mori, S., Morita, T., Pepper, W., Pitcher, H., Price, L., Raihi, K., Roehrl, A., Rogner, H.-H., Sankovski, A., Schlesinger, M., Shukla, P., Smith, S., Swart, R., van Rooijen, S., Victor, N., Dadi, Z., 2000. IPCC Special Report on Emissions Scenarios. Cambridge University Press, Cambridge, UK and New York, p. 599.

Nash, J.E., Sutcliffe, J.V., 1970. River flow forecasting through conceptual models part I—a discussion of principles. J. Hydrol. 10 (3), 282–290.

Nie, L., Lindholm, O., Lindholm, G., Syversen, E., 2009. Impacts of climate change on urban drainage systems – a case study in Fredrikstad, Norway. Urban Water J. 6 (4), 323–332.

ÖWAV, 2007. Directives of the Austrian Society for Water and Waste Management (ÖWAV), p. 47, Austrian Society for Water and Waste Management (ÖWAV).

ÖWAV, 2020. ÖWAV-Positionspapier: Positionen und Forderungen der Wasserwirtschaft in Österreich 2020.

Owens, J.H., Miltner, R.J., Rice, E.W., Johnson, C.H., Dahling, D.R., Schaefer, F.W., Shukairy, H.M., 2000. Pilot-scale ozone inactivation of Cryptosporidium and other microorganisms in natural water. Ozone Sci. Eng. 22 (5), 501–517.

Parajka, J., Blaschke, A.P., Bloschl, G., Haslinger, K., Hepp, G., Laaha, G., Schoner, W., Trautvetter, H., Viglione, A., Zessner, M., 2016. Uncertainty contributions to low-flow projections in Austria. Hydrol. Earth Syst. Sci. 20 (5), 2085–2101.

Paraskeva, P., Graham, N.J.D., 2002. Ozonation of municipal wastewater effluents. Water Environment Research 74 (6) (569–581(513)).

Pazwash, H., 2016. Newer Trends in Storm Water Management (Green Infrastructure). Urban Storm Water Management, 2nd Edition, 479-544.

Reischer, G.H., Haider, J.M., Sommer, R., Stadler, H., Keiblinger, K.M., Hornek, R., Zerobin, W., Mach, R.L., Farnleitner, A.H., 2008. Quantitative microbial faecal source tracking with sampling guided by hydrological catchment dynamics. Environ. Microbiol. 10 (10), 2598–2608.

Reszler, C., Blöschl, G., Komma, J., 2008. Identifying runoff routing parameters for operational flood forecasting in small to medium sized catchments/Identification de paramètres de propagation d'écoulement pour la prévision opérationnelle de crue au sein de bassins versants de petite à moyenne taille. Hydrological Sciences Journal/Journal des Sciences Hydrologiques 53, 112–129.

Rickert, B., Chorus, I., Schmoll, O. (Eds.), 2016. Protecting Surface Water for Health. Identifying, Assessing and Managing Drinking-water Quality Risks in Surface-water Catchments. World Health Organization 178 pages.

Schijven, J., Derx, J., Husman, A.M.D., Blaschke, A.P., Farnleitner, A.H., 2015. QMRAcatch: microbial quality simulation of water resources including infection risk assessment. J. Environ. Qual. 44 (5), 1491–1502.

Schreiber, H., Behrendt, H., Constantinescu, L.T., Cvitanic, I., Drumea, D., Jabucar, D., Juran, S., Pataki, B., Snishko, S., Zessner, M., 2005. Nutrient emissions from diffuse and point sources into the River Danube and its main tributaries for the period of 1998–2000 – results and problems. Water Sci. Technol. 51 (3–4), 283–290.

Signor, R.S., Ashbolt, N.J., 2009. Comparing probabilistic microbial risk assessments for drinking water against daily rather than annualised infection probability targets. J. Water Health 7 (4), 535–543.

Sokolova, E., Astrom, J., Pettersson, T.J., Bergstedt, O., Hermansson, M., 2012. Decay of Bacteroidales genetic markers in relation to traditional fecal indicators for water quality modeling of drinking water sources. Environ Sci Technol 46 (2), 892–900.

Sokolova, E., Petterson, S.R., Dienus, O., Nystrom, F., Lindgren, P.E., Pettersson, T.J., 2015. Microbial risk assessment of drinking water based on hydrodynamic modelling of pathogen concentrations in source water. Sci. Total Environ. 526, 177–186.

Soller, J.A., Schoen, M.E., Varghese, A., Ichida, A.M., Boehm, A.B., Eftim, S., Ashbolt, N.J., Ravenscroft, J.E., 2014. Human health risk implications of multiple sources of faecal indicator bacteria in a recreational waterbody. Water Res. 66, 254–264.

Standhartinger, S., Godina, R., 2013. Mitteilungsblatt des Hydrographischen Dienstes in Österreich. Müller, G., Godina, R., Fuchs, G., Lorenz, P. and Weilguni, V. (eds), Bundesministerium für Land- und Forstwirtschaft, Umwelt und Wasserwirtschaft Abt. VII 3 Wasserhaushalt, Vienna, Austria.

Stapleton, C.M., Kay, D., Magill, S.H., Wyer, M.D., Davies, C., Watkins, J., Kay, C., McDonald, A.T., Crowther, J., 2011. Quantitative microbial source apportionment as a tool in aiding the identification of microbial risk factors in shellfish harvesting waters: the Loch Etive case study. Aquac. Res. 42 (s1), 1–20.

Sterk, A., de Man, H., Schijven, J.F., de Nijs, T., de Roda Husman, A.M., 2016. Climate change impact on infection risks during bathing downstream of sewage emissions from CSOs or WWTPs. Water Res. 105, 11–21.

Szolgay, J., 2004. Multilinear flood routing using variable travel-time discharge relationships on the Hron River. J. Hydro. Hydromech. 52.

Taghipour, M., Shakibaeinia, A., Sylvestre, É., Tolouei, S., Dorner, S., 2019. Microbial risk associated with CSOs upstream of drinking water sources in a transboundary river using hydrodynamic and water quality modeling. Sci. Total Environ. 683, 547–558.

Teunis, P.F., Havelaar, A.H., 2000. The Beta Poisson dose-response model is not a single-hit model. Risk Anal. 20 (4), 513–520.

Teunis, P.F., van der Heijden, O.G., van der Giessen, J.W.B., Havelaar, A.H., 1996. The Dose-Response Relation in Human Volunteers for Gastro-Intestinal Pathogens. National Institute for Public Health and the Environment (RIVM) RIVM Report 284550002.

Teunis, P.F., Moe, C.L., Liu, P., Miller, S.E., Lindesmith, L., Baric, R.S., Le Pendu, J., Calderon, R.L., 2008. Norwalk virus: how infectious is it? J. Med. Virol. 80 (8), 1468–1476.

van Vuuren, D.P., Edmonds, J., Kainuma, M., Riahi, K., Thomson, A., Hibbard, K., Hurtt, G.C., Kram, T., Krey, V., Lamarque, J.-F., Masui, T., Meinshausen, M., Nakicenovic, N., Smith,

S.J., Rose, S.K., 2011. The representative concentration pathways: an overview. Clim. Chang. 109 (1), 5.
Walter, R., Rüdiger, S., 1981. Ein Zweistufenverfahren zur Virusanreicherung aus Lösungen mit geringem Virustiter. J. of Hygiene, Epidemiology. Microbiol. Immunol. 25, 71–81.
Ward, R.L., Bernstein, D.I., Young, E.C., Sherwood, J.R., Knowlton, D.R., Schiff, G.M., 1986. Human rotavirus studies in volunteers - determination of infectious dose and serological response to infection. J. Infect. Dis. 154 (5), 871–880.
WHO (Ed.), 2017a. Climate Resilient Water Safety Plans: Managing the Health Risks Associated With Climate Variability and Change. Organization, World Health.
WHO (Ed.), 2017b. Guidelines for Drinking-water Quality: Fourth Edition Incorporating the First Addendum. Organisation, World Health.
Willems, P., Olsson, J., Arnbjerg-Nielsen, K., Beecham, S., Pathirana, A., Bülow Gregersen, I., Madsen, H., Nguyen, V.-T.-V., 2012. Impacts of Climate Change on Rainfall Extremes and Urban Drainage Systems. IWA Publishing, London, UK.
Willmott, C.J., Matsuura, K., 2005. Advantages of the mean absolute error (MAE) over the root mean square error (RMSE) in assessing average model performance. Clim. Res. 30, 79–82.
Zhang, Q., Gallard, J., Wu, B.L., Harwood, V.J., Sadowsky, M.J., Hamilton, K.A., Ahmed, W., 2019. Synergy between quantitative microbial source tracking (qMST) and quantitative microbial risk assessment (QMRA): a review and prospectus. Environ. Int. 130, 10.